Diliana Maria Barradas Rebelo dos Santos

Master's in Biomedical Engineering

Human Activity Recognition for an Intelligent Knee Orthosis

Dissertação para obtenção do Grau de Mestre em
Engenharia Biomédica

Orientador : Hugo Filipe Silveira Gamboa, Prof. Auxiliar, Faculdade de Ciências e Tecnologias da Universidade Nova de Lisboa

Co-orientadores : Christoph Amma, phD Student, Cognitive Systems Lab, Karlsruhe Institute of Technology, Germany
Tanja Schultz, Profª. Catedrático, Cognitive Systems Lab, Karlsruhe Institute of Technology, Germany and Carnegie Mellon University, Pittsburg, USA

Júri:

Presidente: Doutor Pedro Manuel Cardoso Vieira

Arguente: Doutora Ana Luísa Nobre Fred

Vogal: Doutor Hugo Filipe Silveira Gamboa

FACULDADE DE CIÊNCIAS E TECNOLOGIA
UNIVERSIDADE NOVA DE LISBOA

September, 2012

Human Activity Recognition for an Intelligent Knee Orthosis

Acknowledgements

First and foremost, I offer my sincerest gratitude to my supervisor, Professor Hugo Gamboa, who has supported me throughout my thesis with his patience and knowledge whilst allowing me the room to work in my own way. I attribute the level of my Masters degree to his encouragement and effort and without him this thesis, too, would not have been completed.

This project would not have been possible either without my stay in Karlsruhe, in *CSL-Cognitive Systems Lab* of the *KIT-Karlsruhe Institute of Technology* under Dr.Tanja Scultz's guidance. To you, Dr.Tanja Scultz, I thank you for the wonderful reception, environment and knowledge your laboratory offered me. To my co-supervisor, PhD student Christoph Amma, my biggest acknowledgement for the extreme patience to fulfil all of my questions and needs, to polish my failures and to be available 24/7.

In my daily work I have been blessed with a friendly and cheerful group of fellow students. I would like to thank all of my *CSL*-friends, Mark, Thang, Dominic T., George, Tim, Dario, Dirk, Dominic H., Christian, Matthias, Michael, Daniel L., Daniel, Lena, Zlatka, and every others and to my friend from India, Melvin, for making my time in Germany one of the best in my life. Back in Portugal, the daily presence of my dearest friends Rodolfo, Ângela, Ricardo and Nuno was crucial whether for the funny moments and adventures or for the constant available support.
I shall thank you with all of my heart.

I also want to underline the primordial role of all of the excellency professionals from *PLUX-Wireless Biosignals, S.A.*, who welcomed me and supported me along my thesis.

Por último, mas não por importância, quero agradecer à minha mãe Cesaltina, ao meu pai Manuel e às minhas irmãs, Dinamene e Diana, por todo o incansável apoio especialmente ao longo destes meses e por nunca deixarem de acreditar em mim ou sequer permitirem que eu própria o fizesse.

Abstract

Activity recognition with body-worn sensors is a large and growing field of research. In this thesis we evaluate the possibility to recognize human activities based on data from biosignal sensors solely placed on or under an existing passive knee orthosis, which will produce the needed information to integrate sensors into the orthosis in the future.

The development of active orthotic knee devices will allow population to ambulate in a more natural, efficient and less painful manner than they might with a traditional orthosis. Thus, the term *'active orthosis'* refers to a device intended to increase the ambulatory ability of a person suffering from a knee pathology by applying forces to correct the position only when necessary and thereby make usable over longer periods of time.

The contribution of this work is the evaluation of the ability to recognize activities with these restrictions on sensor placement as well as providing a proof-of-concept for the development of an activity recognition system for an intelligent orthosis.

We use accelerometers and a goniometer placed on the orthosis and Electromyography (EMG) sensors placed on the skin under the orthosis to measure motion and muscle activity respectively. We segment signals in motion primitives semi-automatically and apply Hidden-Markov-Models (HMM) to classify the isolated motion primitives. We discriminate between seven activities like for example walking stairs up and ascend a hill. In a user study with six participants, we evaluate the systems performance for each of the different biosignal modalities alone as well as the combinations of them. For the best performing combination, we reach an average person-dependent accuracy of 98% and a person-independent accuracy of 79%.

Keywords: Biosignals, Human activity recognition, Signal-processing, Hidden Markov Models

Resumo

O reconhecimento de actividade humana com sensores corporais é um vasto e promissor campo de investigação. Ao longo deste projecto de mestrado, avaliamos a possibilidade de reconhecimento de movimento humano através do estudo de biosinais captados por sensores localizados directamente numa ortótese do joelho ou na pele, o que permitirá obter a informação necessária para se proceder à integração futura destes sensores no próprio dispositivo.

O desenvolvimento de dispositivos ortóticos activos do joelho proporcionará à população doente um meio de locomoção mais natural, eficiente e menos dolorosa quando comparado com os tradicionais. O termo *'ortótese activa'* refere-se ao dispositivo cuja função é melhorar a capacidade de movimento de uma pessoa que sofre de uma patologia do joelho recorrendo à aplicação de uma força somente quando necessária o que leva ao seu uso por um maior período de tempo.

Este trabalho contribuirá para o desenvolvimento da área de reconhecimento de actividade humana na vertente de possibilidade de criação de equipamentos médicos inteligentes com sensores incorporados.

Sob a ortótese, dispomos os acelerómetros e o goniómetro e, sob a pele, são colocados os eléctrodos de electromiografia de superfície de modo a captar movimento e actividade muscular, respectivamente. Quanto à metodologia, os sinais são repartidos semi-automáticamente em ciclos que, após a extracção de características, constituem a entrada para o classificador supervisionado escolhido, HMM. Num estudo desempenhado por seis participantes, investigámos qual o grau de identificação dos movimentos bem como qual ou quais as combinações de sinais com maior precisão. Para a melhor combinação, obtivémos um rigor de 98% num contexto sujeito-dependente e 79% para o caso de sujeito-independente.

Palavras-chave: Biosinais, Reconhecimento de actividade humana, Processamento de sinal, HMM

Contents

List of Figures

List of Tables

Listings

ACC Accelerometry

EMG Electromyography

GON Goniometry

HMM Hidden-Markov-Models

GMM Gaussian Mixture Model

MCL Medial Collateral Ligament

LCL Lateral Collateral Ligament

ACL Anterior Collateral Ligament

PCL Posterior Collateral Ligament

ROM Range of Motion

EM Expectation Maximization

MCFS Multi Channel Feature Sequence

FS Feature Sequence

EMG&GON Electromyography and Goniometry

GON&ACC Goniometry and Accelerometry

EMG&ACC Electromyography and Accelerometry

EMG&GON&ACC Electromyography, Goniometry and Accelerometry

ECG Electrocardiography

EEG Electroencephalography

1

Introduction

1.1 Motivation

Passive orthoses are widely used for conservative therapy of diseases like Gonarthrosis, which is Osteoarthritis in the knee joint. Depending on the type of arthrosis, these orthoses apply a constant force on the knee joint to correct a defective position. This is usually painful or at least unpleasant for the wearer after a certain amount of time. Future active orthoses could be able to vary this force depending on the current wearers activity and therefore only apply force if the knee joint is stressed, e.g. while walking stairs but not while the wearer is sitting. This will impose less strain on the wearer. In order to develop such an active orthosis it is necessary to robustly recognize the users activity, which is the topic of this thesis.

Briefly, we can summarize the motivation of this work in two questions:

- How can we improve the patient's daily life quality?
- How can we rely on biomechanical signals for human activity recognition?

1.2 Objectives

The primary objective of this thesis is to investigate the possibility to classify human activities from biosignal sensors integrated into a knee orthosis and how well we can discriminate isolated motion primitives. An orthosis that is capable to recognize its wearers activity would be able to adapt itself to the users' situation for enhanced comfort. We use a setup with three biosignal modalities: electromyography (EMG), goniometry (GON) and accelerometry (ACC) to measure motion and muscle activity of the knee. Another

objective of this thesis is to state which signal (or combination of signals) provide higher classification accuracy.

In order to fulfill these goals, we used a methodology based on pattern recognition and HMM as classifier. The procedure is explained on chapters 5 and 6.

The contribution of this work is the evaluation of the ability to recognize activities with these restrictions on sensor placement as well as providing a proof-of-concept for the development of an activity recognition system for an intelligent orthosis.

1.3 Thesis Overview

This thesis is organized in seven chapters and one appendix, as represented in figure 1.1.

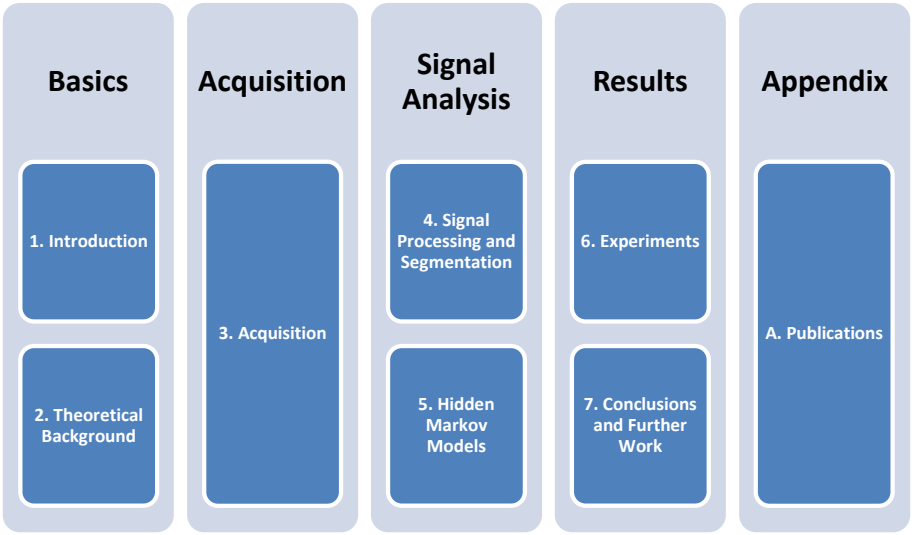

Figure 1.1: Thesis' overview diagram

This first chapter introduces the theme and motivation to the reader, explaining the objectives and importance of the developed work. It has the goal to contextualize the reader giving a thesis overview. Next, in Chapter 2, the theoretical concepts are presented as well as the state of the art. These two chapters form the basic structure for the overall work.

The second block consists in just one chapter, *Acquisition*, where the procedure for signal recording is detailed. Each one of the six subjects had EMG sensors placed on the skin and wore a passive orthosis with GON and ACC sensors placed on it and performed the activities' acquisition protocol. This chapter concerns the collection of data.

Chapter 4 discusses the acquired raw signals and clarify the algorithm for semi-automatic segmentation. Plus, the total structure of our final database is presented. In Chapter 5 the HMM decoding used in this project is introduced as well as the main differences compared to a standard HMM. These two chapters fix up the third block named *Signal Analysis*.

The *Results* set consists of chapter 6 and chapter 7. Chapter 6 presents a detailed description of the performed experiments together with a discussion of the results. As a continuation, chapter 7 resumes our work by presenting the main conclusions and further work.

The thesis has one additional appendix which contains the papers published during this project: *Clustering Algorithm for Human Behaviour Recognition based on Biosignals Analysis*, accepted as a book chapter in *Human Behaviour Recognition Technologies: Intelligent Applications for Monitoring and Security* and *Human Activity Recognition for an Intelligent Knee Orthosis* submitted to the *2013 Biosignals Conference*.

The implemented algorithms were develop using *Python*, *Eclipse* and the *BioKit* toolbox. In order to create our database, we used *SQLAlchemy*.

2

Theoretical Background

The purpose of this chapter is to contextualize the reader about the main subject of this work. Through the subchapters, we will introduce the knee anatomy, biomechanical signals acquisition and processing, classification algorithms and literature review.

2.1 Knee Anatomy

2.1.1 Essential Concepts

The knee joint combines several bones, muscles and ligaments. As a short approach, it integrates three bones: *femur*, which is the thigh large bone attached by ligaments to the *tibia* and the *patella* (or kneecap), that slides on the knee as it bends (see figures 2.1,2.2 and 2.3). There are also a number of ligaments, cartilages and muscles which strengthen and support the knee [1]. Basically, the knee can be thought of having four ligaments which stabilize it [1]:

1. Medial Collateral Ligament (MCL): Runs along the inner part of the knee and prevents bending inwards;

2. Lateral Collateral Ligament (LCL): Runs along the outer part of the knee and prevents bending outwards;

3. Anterior Collateral Ligament (ACL): Lies in the middle of the knee and prevents the tibia sliding forwards in front of the femur. It also provides rotational stability;

4. Posterior Collateral Ligament (PCL): In conjunction with ACL, it prevents the tibia sliding backwards under the femur.

Meniscus

The meniscus is a wedge-like cushion which connects the bones of the knee together. The cartilages are shaped in a form that provides a strong stabilization. It helps the weight support and it also interferes in sliding and turning in many direction. It also acts as a shock absorber and keeps the thigh bone and shin bones from grinding against each other.

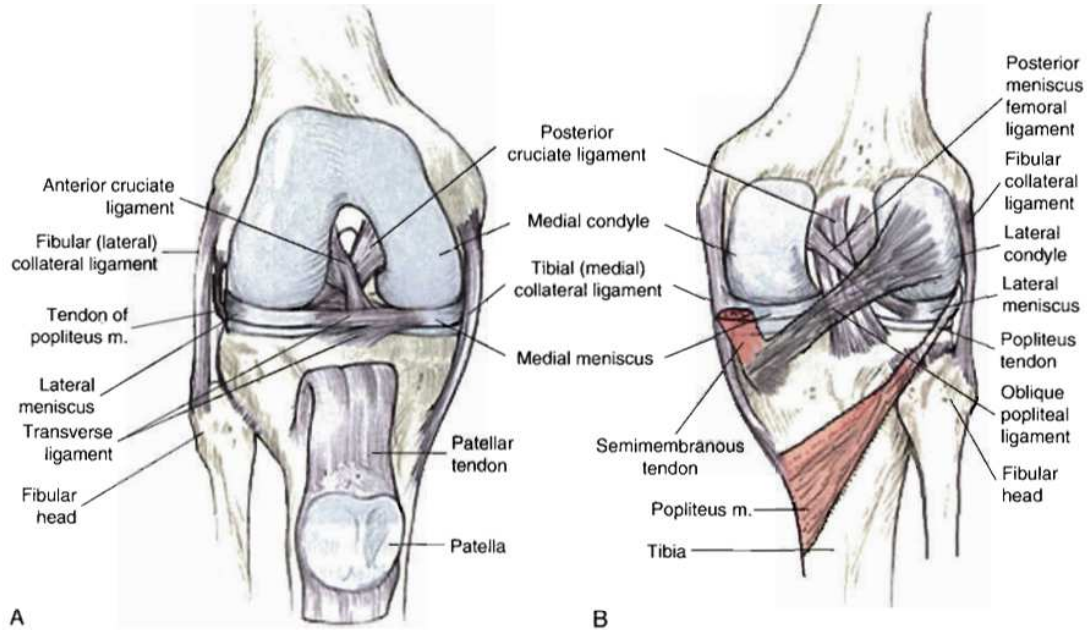

Figure 2.1: Knee anterior (A) and posterior (B) view [1]

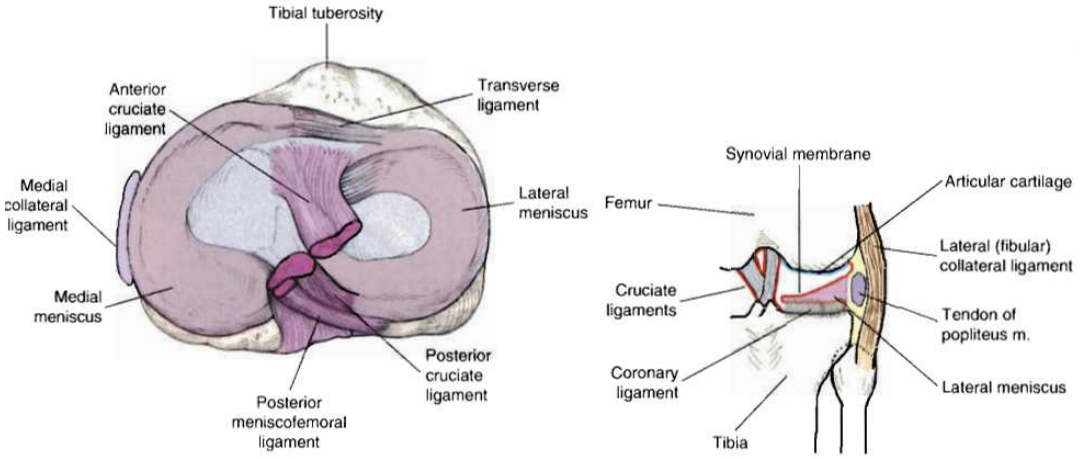

Figure 2.2: Superior end of the right tibia [1]

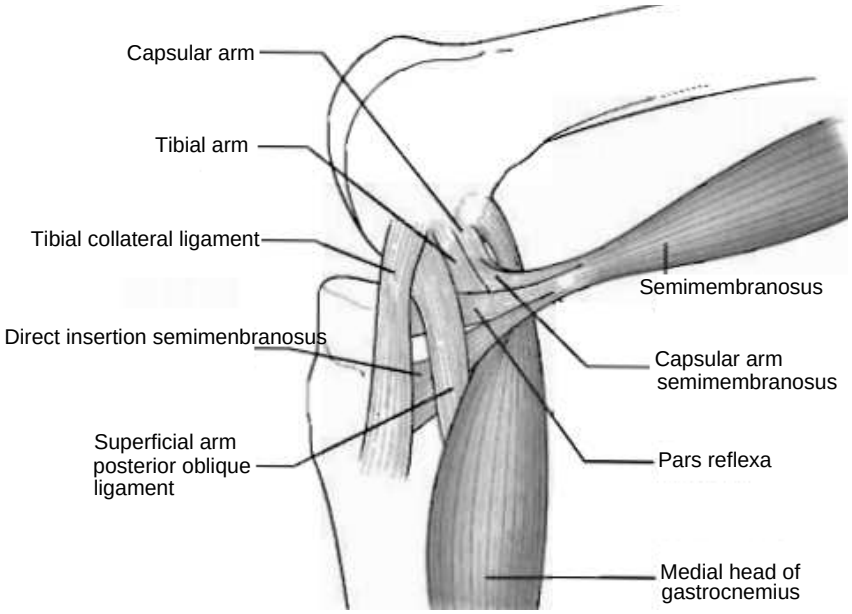

Figure 2.3: Knee supporting structures diagram [1]

2.1.2 Muscles

2.1.2.1 Quadriceps: Extensor muscles

The extensor knee muscle group is the *quadriceps*. As the name suggests, it has four "components": *anterior rectum*, *vastus lateralis*, *vastus medialis* and *vastus intermedius*, which converge to a distal insertion at the patella and tibia's anterior tuberosity. Quadriceps are responsible for knee extension.The *vastus medialis* is responsible for medial rotation and, *vastus lateralis* for lateral rotation [9].

2.1.2.2 Hamstring: Flexor muscles

Hamstring is the muscle complex responsible for flexion. It consists of a combination of three small but long muscles: *femoral biceps*, *semitendinosus* and *semimembranosus* muscles [9].

Femoral biceps It begins at the ischial tuberosity and at the lateral lip of the linea aspera of the femur converging to the fibular head. This muscle performs extension by adduction and external rotation and, flexion by external rotation of the knee. It also provides pelvic retroversion.

Semitendinosus muscle Semitendinosus muscle also begins at the ischial tuberosity next to the femoral biceps and converges to the tibial tuberosity. It is responsible for hip extension, helps in internal rotation and adduction as well as performing flexion and medial rotation of the knee. If the lower limbs are fixed, semitendinosus muscle provides pelvis retroversion.

Semimembranosus muscle Analogously to femoral biceps and semitendinosus muscle, the semimembranosus muscle has origin at the ischial tuberosity. Nevertheless, its

insertion is in the proximal tibia by fascia of the popliteal muscle. It performs extension, adduction and hip internal rotation as well as flexion and internal rotation of the knee.

2.1.2.3 Gastrocnemius: Flexor muscle

The gastrocnemius is a large muscle located in the lower leg forming part of the calf and participates directly on the flexion of the knee. Its purpose is to push the leg down when required during activities such as walking, jogging or even just standing. It also allows plantar flexion of the foot, which is important in a number of different activities.

The gastrocnemius originates toward the bottom of the femur and inserts at the Achilles tendon.

The figure 2.4 illustrates all of the three muscle complexes aforementioned.

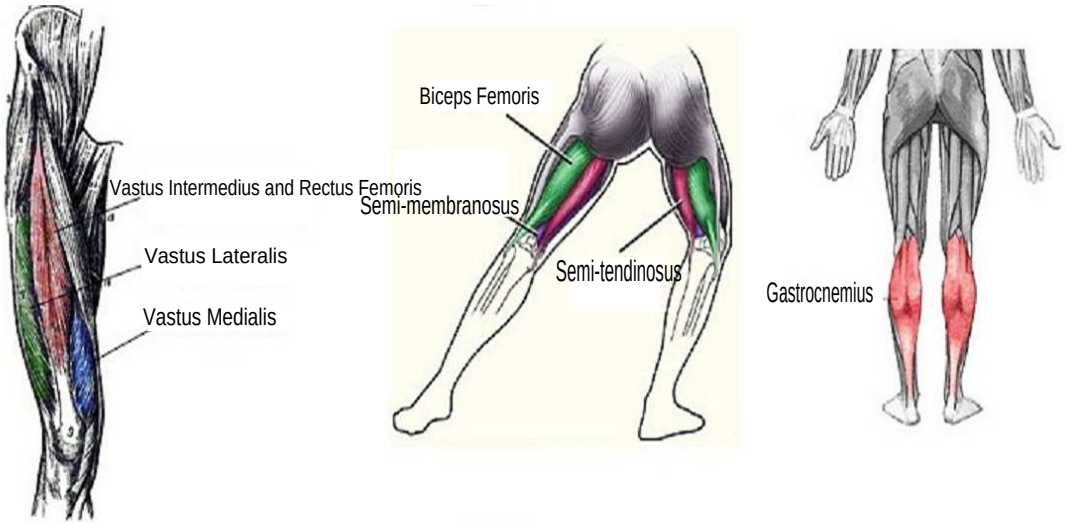

Figure 2.4: Knee extensors and flexors muscles [2,3]

2.1.3 Pathology: Gonarthrosis

Osteoarthritis is a joint inflammation that results from cartilage degeneration and it can be caused by aging, heredity and injury from trauma or disease. This pathology is degenerative and it can be characterized by the progressive destruction of joint cartilage, bone sclerosis and osteochondral proliferation, which results in a painful movement or progressive functional movement impotence.

Gonarthrosis is osteoarthritis in the knee.

Patients with gonarthrosis are confronted with a variety of therapy options. For example, the use of orthosis is a non surgical option. The orthoses are designed to apply an external moment during gait so the load on the knee compartment might be diminished. However, as a disadvantage for patients, this applied force is constant even when it is not needed, which may cause them pain. Figure 2.5 shows an x-ray to a healthy knee and a knee with gonarthrosis.

Figure 2.5: X-ray of a normal knee with space between the bone of the upper and lower leg (A). (B) shows bone spurs and a narrowed joint space caused by osteoarthritis [4]

2.2 Introduction to biosignals

Biosignal monitoring and recording is the extension of medical investigations taking into consideration the development over time. A biosignal is a term applied to all signals continuously captured from biological sources. Each kind may be related to a specific event so they are usually categorized as [10–12]:

- **Bioelectrical signals:** Bioelectric signals are formed in cells and organs by nerve cells, mainly in the heart and the brain. Its source is the cell membrane and it propagates as an action potential. They are very low amplitude and low frequency;
- **Biomechanical signals:** This type represents all signals from some biological movement source such as motion, force, pressure or flow;
- **Biomagnetic signals:** The concept of biomagnetic signals is inborn in the electric human nature and it is associated to the measurement of magnetic fields in some organs (e.g, brain);
- **Bioacoustics signals:** Many biomedical phenomena have an acoustic nature. Bioacoustics signals raise from the attainment of this events such as blood flow or digestive noises. The one primary acoustic signal is speech and sound produced by the vocal tract.

In this work, a biosignal can be also referred as *time series*. A time series is a sequence of observations of a variable over time. Each one of the aforementioned signals can be whether deterministic or stochastic, depending on its probabilistic character. *Deterministic signals* are those that might be described by mathematical functions and they can be subdivided in periodic, quasi-periodic and transient. A signal is *periodic* if it completes a pattern within a measurable time frame T called a period and repeats that pattern over

identical subsequent periods. Thus, considering $x(t)$ a periodic signal, it can be described as:

$$x(t) = x(t + kT) \tag{2.1}$$

where k is an integer.

The quasi-periodic group is the most common type and it refers to signals that present some similarity to a periodic function but do not meet the strict definition. A transient signal usually presents high-amplitude and short-duration. As examples, a sine wave is the perfect example of a periodic signal, an Electrocardiography (ECG) exam is the quasi-periodic representative and, a cell response illustrates the third class.

On the other hand, a *stochastic signal* can be defined as a statistical phenomenon that evolves in time according to probabilistic laws and can be divided into stationary, if its probability distribution does not change when shifted in space or time, or non-stationary categories. As examples, brain alpha waves represent a stationary time series while an Electroencephalography (EEG) exam illustrates the second referred label. These relationships are exhibited on figure 2.6.

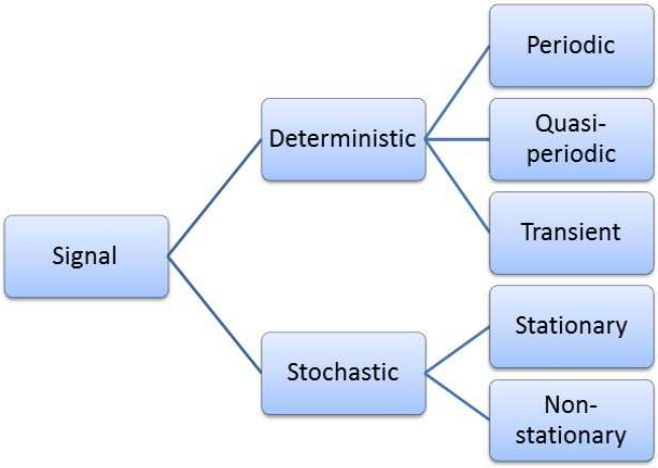

Figure 2.6: Signal classification

2.3 Methods of sensing biosignals

In this section, only the activity recognition's biosignals used in this project will be addressed: EMG, GON and ACC.

2.3.1 EMG

The human skeletal muscle is formed by cylindrical individual cells (named fibers) joined together by connective tissue.
Muscles are forced to contract once they receive a stimulus from the motor nerve. These nerves are responsible for the transport of information as nervous impulses from the

brain or spinal cord to skeletal muscles. In order to reach the muscle, each axon (or nervous fiber) suffers ramifications and enervations into manifold muscle individual fibers. Although one motor neuron may innervate several muscle fibers, each fiber is innervated by only one motor neuron. A motor unit can be defined as a group of muscle fibres and their innervating terminal branches of one fibre whose cell body is located in the anterior horn of the spinal gray matter. Thus, when a neuron is activated, all of its enervated fibers respond to the impulse which causes its own electric signal and, consequently, leads to contraction. Although the electric impulse created and conducted by each fiber is too low (less than $100mV$), when several fibers transport the impulse simultaneously, they form sufficient voltage that can be detected on the surface of the skin by a pair of electrodes. The detection, amplification and recording of these potential differences produced by the contraction of the skeletal muscle is called EMG.

In this research, the EMG is obtained according to a non-invasive method, by placing the electrodes on the skin, as can be seen in 2.7.

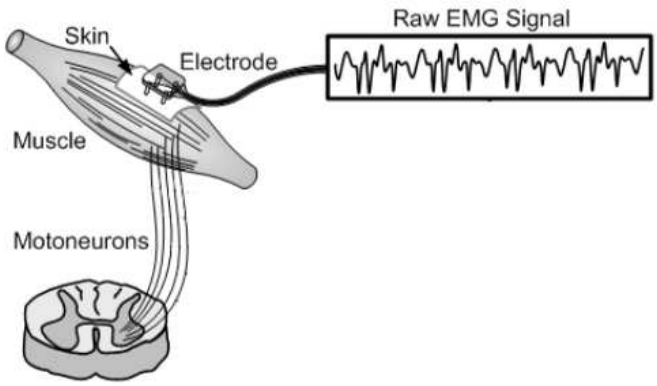

Figure 2.7: EMG acquisition, with an electrode placed on the skin, and example of a raw signal [5]

From EMG's analysis, it is possible to detect clinical abnormalities, level of activation, recruitment order or to evaluate movement biomechanics.

2.3.2 GON

In Medicine, GON is a method directly related to measure and document initial and subsequent joint's angles.

A goniometer is a device used to quantify joint angles. Figure 2.8 shows the goniometer sensor used in this work from Biometrics Ldt[1]. This device is designed to measure rotations in two planes. When applied to the knee, the goniometer is capable to detect flexion/extension and valgus/varus. In this work, this sensor was used to measure the angle of the knee joint over time.

[1] http://www.biometricsltd.com

The maximum available angle range is defined as the Range of Motion (ROM) allowed at a joint and it is usually measured by the number of degrees from the starting to the ending position of a segment considering its full range of movement [13].

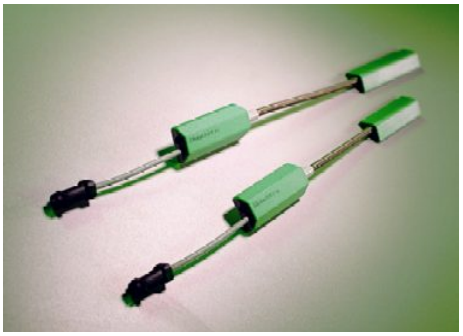

Figure 2.8: The figure represents two goniometers from Biometrics Ldt.

2.3.3 ACC

The ACC is a common procedure for kinematic and motion analysis. Motion can be quantified with an accelerometer which measures acceleration relative to itself. Hence, the signal from accelerometers may be used as motion detectors [14] or recognition [15] as well as for body-position and posture sensing [16]. A triaxial accelerometer is a sensor capable to estimate the value of acceleration along the x,y and z axes; it measures acceleration relative to free fall as well as its magnitude and direction, as a vector quantity. The output can be used to sense position, for example. In the context of this work, each one of the accelerometers presented the coordinate system shown in figure 2.9.

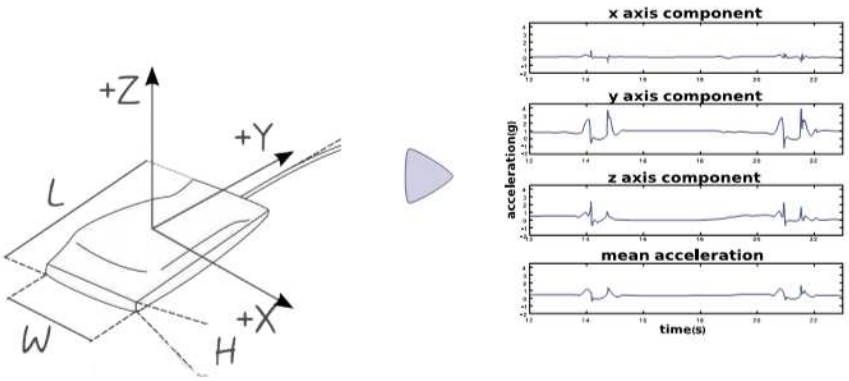

Figure 2.9: Accelerometer axis representation and acquired signals [6]. This pictures also shows the sensors' length (L), width (W) and height (H).

According to the figure, the acquired signals present positive, negative or neutral voltage values which correspond, respectively, to a positive, negative or neutral proportional acceleration.
In order to calibrate the gain and zero offset of an accelerometer, it must be kept in mind

that, at rest, the sensor with its sensitive axis pointing towards the center of the Earth present $1g$ as result, which concerns to gravity.

2.4 Biosignal pattern recognition and Classification

Biosignal pattern recognition concerns a group of measures applicable in biomedical signal processing. This phase involves all the stages from data acquisition to identification of the pattern and its usage for classification, detection or parameter estimation of the input value and machine's comprehension of previous results or concepts obtained from feature extraction, feature selection, clustering and classification, detection or parameter estimation, which is important for learning [17].

Classification is the allocation of a label to an input value: assuming known the number of possible labels in a given data, the aim is to establish a rule whereby we can classify new examples into one of the existing classes (Supervised Learning) which can be accomplished, depending on the problem, by different types of algorithms: logic-based, perceptron-based, instance-based or statistical algorithms [18]. On the contrary, Unsupervised Learning or Clustering occurs when the aim is to discover the existence of classes or clusters in a given set of observations, without a priori labelling.

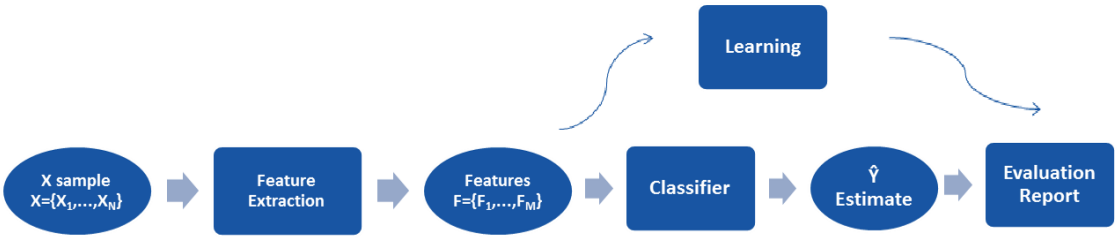

Figure 2.10: Classification theory scheme

Figure 2.10 represents a classification scheme of a statistical learning algorithm: given a sample x, the classifier "reads" its characteristics and assigns it to a class. As supervised learning, each sample has a respective label, Y, which is already known. The X represents a sample with $X = X_1, \ldots, X_N$ where N is the number of acquired channels. After features extraction, each sample has a group of attributes, $F = F_1, \ldots, F_M$ where M is the number of features.

So the classification is well accomplished, the classifier needs to calculate $p(Y|X)$ which is the probability of the class is Y knowing that the sample is X. To do it, it also determines $p(X|Y)$, the probability of the sample is X knowing that the class is Y. Ideally, the recognizer output, $\check{Y}$,is equal to Y.

The accuracy is one possible method to evaluate the performance of a classifier and it consists on the degree of closeness between the measured value and its true value. Thus, it is represented as the proportion of correct classifications for a randomly selected

instance, i.e, is the percentage of well classified data in the testing data set.

$$\text{Accuracy or Recognition Rate} = \frac{\textit{Number of correct classifications}}{\textit{All tested cases}} \tag{2.2}$$

However, this can also be expressed in terms of the errors

$$\text{Error Rate} = \frac{\textit{Number of wrong classifications}}{\textit{All tested cases}} \tag{2.3}$$

Nevertheless, the correct error value is never known since it is impossible to test the classifier with all possible examples. Even so, for limited data, one possible technique is the leave-one-out cross-validation. *Cross-validation* is an evaluation method that involves partitioning the initial data into complementary subsets , performing the analysis on one subset, the *train set*, and validating the analysis on the other subset, the *test set* or *validation set*. When the validation set has only one sample and the remaining data is used for training, the method is called *leave-one-out cross-validation* [19].

2.4.1 Hidden Markov Models (HMM)

Hidden Markov Models (HMM) are a very powerful tool that statistically models a process that varies in time [20]. They are stochastic methods that use temporal information to model a sequence of observations. They are organized in a finite set of states, each of which is associated with a probability distribution, generally multidimensional. Transitions among the states are defined by a set of *transition probabilities*. Each state has probability function associated; thus, each state can generate an observation. However, the same sequences of observations can be achieved from different probabilities and from sequences of different states. A model can be described by Equation 2.4,

$$\lambda = \{A, B, \Pi\} = \{a_{i,j}, b_i, \pi_i\},\ i, j = 1, \ldots, N \tag{2.4}$$

where:

- A=$\{a_{i,j}\}$ is the transitions probability matrix between state i and j (and N the number of states);
- B=$\{b_i\}$ represents the matrix of all emission probabilities of the state i. Considering a continuous distribution, this matrix refers to a probability density function;
- Π=$\{\pi_i\}$ represents the matrix with the probabilities of a model being initialized from the state i.

Given the form of HMM, there are three items to consider so the model is useful in real applications. These points are the following:

1. Adjustment of the model parameters to maximize the probability of a certain model given the observation sequence (learning the model).

2. Computation of the probability for the observation sequence, given the model;
3. Resolution of the most likely sequence of states that best explains the observations;

Figure 2.11 illustrates a simple HMM with a left-to-right topology.

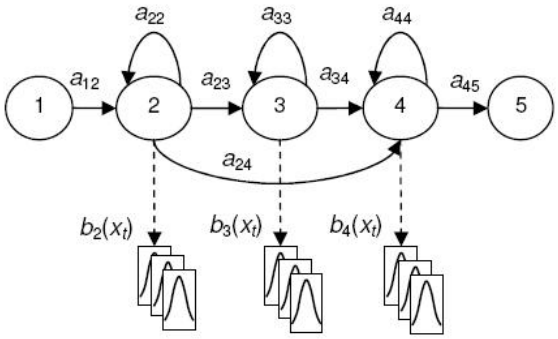

Figure 2.11: HMM model with left-to-right topology with three emissors states [7]

The main goal is to determine the sequence of states that maximizes the posterior probability. To do that, the *Viterbi algorithm* [20] is applied: computes the most likely state sequence for time step. This algorithm is responsible for finding the *Viterbi path* (most likely sequence of hidden states) in a sequence of observed events.

2.5 State of the Art

Activity recognition concerns the automatic identification of types of physical activity from a set of measurements which can contain data from devices such video cameras, pedometers, heart rate monitors, accelerometers, EDA sensors, goniometers, EMG sensors, among others. Although activity recognition can be easily achieved by humans, in order to program it, automatic classification needs to improve itself considering classes and accuracy. Even so, the advantages are still relevant mainly because direct classification of visual data is expensive, very time-consuming and depends on the subjects as well as the recording environment.

The constant pursuit of electrophysiologic knowledge led to various experiments or studies in which several techniques and models were developed. In this section are presented and discussed some of these studies, which results or limitations can be used as a start point for new research, structured by themes: work on gait, activity analysis and recognition as well as classification methods.

The intuitive procedure to evaluate human motion comes from the direct observation of movement which can be obtained from video camera data analysis. In [21], Boesnach et al. present a new procedure to model human motion based on $3D$ joint features reconstruction of daily activities such, for example, setting the table with cup and saucer,

pouring water from a coffepot into the cup and stirring the water in the cup with a coffee spoon. The extracted features were used to feed the artificial neural network. The results obtained were compared to those obtained from HMM classifier.

Gait analysis as well as posture are the primers subjects to investigate in health domain [22–24]. Gait analysis studies involves continuous curves of data measured over a gait cycle [25]. In order to deliver a proper report, health technicians need to compare the exam results with statistical proved normal data. In [25] several tools to process statistical gait data are described.

Once the basic human movement is detected and modelled, different approaches can be applied to analyse different activities. Some studies present different methods or applications on ACC signals, always keeping in mind the goal of activity classification with health purpose. For example, Takeda et al. in [26] exhibits a model possibility based on accelerometers and gyroscopes implemented in a suit so the human activity can be properly measured. Foerster et al. [27] uses a small number of calibrated piezoresistive accelerometers devices to validate the accelerometric evaluation against behaviour observation and conclude about reliability. He proves that wearable accelerometers placed in different parts of the body identify correctly different postures and motions, by comparing the different behaviours and the respective kinematic analysis. In a similar approach, Moe-Nilssen et al. [28] reports a study on a portable system to measure gait parameters which are extracted from a triaxial accelerometer positioned in the lower trunk, during walking. In [29] the use of triaxial accelerometers successfully distinguished between activity (transitions sit-to-stand and stand-to-sit and walk) and rest. In the context of physical activity recognition, in [30], sedentary activities such as sitting or sleeping are discriminated from moderate intensity activities such as walking through the analysis of acceleration data.

Concerning EMG, its analysis is useful for evaluation of muscle activation [31], whether for isolate muscles [32, 33] or joint muscular groups [34]. The use of EMG or electrogoniometers have been applied mostly on kinematics evaluation [23, 35] or on pattern comparisons for diagnosis [36]. Recently, Fleicher et al. [37] prove the importance of muscular activity by presenting a method to determine the joints intended motions through EMG analysis. After the motion is calculated, a leg orthosis can be real-time controlled to sustain patients in daily activities such walking or climbing stairs.

Accurate activity recognition is challenging because human activity is complex and highly diverse. HMM have been used in human motion recognition due to their ability to model sequences that have characteristic temporal evolvement. They have been successfully used for continuous activity recognition whether in video segmentation of activities [21] or continuous gesture recognition [38].

3

Acquisition

This chapter exposes the data acquisition procedure used in this work. Along the different sections, all the acquisition set up is explained: subjects, sensors and protocol.

3.1 Subjects

This work required the participation of one group of volunteer subjects. We performed a study with 6 male subjects. All participants were students and had no known disease related to gait or their knee. Table 3.1 gives anthropometric characteristics on the participants. During the acquisition, all subjects wore shorts and sports shoes. Although the orthosis was not adapted to the anatomy of the subjects, all participants were able to move their knee freely and did not feel any pain. All subjects were shaved on the knee area to increase the quality of the EMG signal and the electrodes' adherence on the skin.

Subject's Statistics	
Height (cm)	181.33 ± 8.16
Weight (kg)	78.17 ± 10.32
Length of femur (cm)	46.17 ± 6.18
Length of tibia (cm)	45.17 ± 2.71

Table 3.1: Means and standard deviations of the anthropometric characteristics of all subjects

3.2 Material and Equipment

3.2.1 Orthosis

This project intends to investigate the possibility to classify isolated human activities from biosignal sensors integrated into a knee orthosis. We created a makeshift intelligent device by equipping a standard Ortema[1] ipomax passive orthosis with sensors. Figure 3.1 illustrates the original equipment.

Figure 3.1: Standard right knee Ortema ipomax passive orthosis

The orthosis itself consists of two rigid shells, one for the upper and one for the lower part of the leg which are fixed to the leg with straps. The shells are connected by a joint on each side in order to allow flexion of the knee joint.

3.2.2 Sensor Layout and Signal Recording

In this research, we equipped the standard orthosis with sensors from PLUX-Wireless Biosignals [2]: two triaxial accelerometers (*xyzPlux*) and one goniometer. Additionally, six EMG sensors (*emgPlux*) to measure muscle activity were put on the skin under the orthosis.
Since all sensors should be integratable into the the orthosis in the future, our setup requires to place all sensors on or under the orthosis.
The orthosis with the full sensor setup can be seen in figure 3.2.

A more detailed description about each sensor layout will be described on the next sections.

3.2.2.1 EMG

Concerning the surface EMG, and according to what was referred in chapter 2, we wanted to acquire signal from six different muscles: *vastus lateralis*, *vastus medialis*, *semitendinosus*,

[1] www.ortema.de
[2] www.plux.info

Figure 3.2: Complete experimental setup: two Bioplux research devices, two ACC (red circles), six EMG and one GON sensors (green arrow) placed on a regular Ortema right knee orthosis

semimembranosus and both parts of the *gastrocnemius*. Hence, six EMG sensors were used on these muscles, under the orthosis. Twelve surface electrodes were placed directly on the skin to acquire muscular activity; plus, the reference electrode was placed on the internal part of the knee, with low percentage of muscles fibres. Figure 3.3 illustrates the placement of the surface electrodes.

Figure 3.3: Placement of EMG surface electrodes

3.2.2.2 GON

One characteristic of a joint is its angular movement. The goniometer has the ability to capture the range of motion over time. However, the crucial aim of its use in this work is related to the angle measurement of the joint during different activities. The goniometer was placed on the joint so it can measure the angle of the orthosis joint which can be assume equal to the angle of the knee joint. Although the goniometer is biaxial only the information from the axis aligned to the degree of freedom of the knee joint was used. Figure 3.4 shows the sensor itself and this scenario.

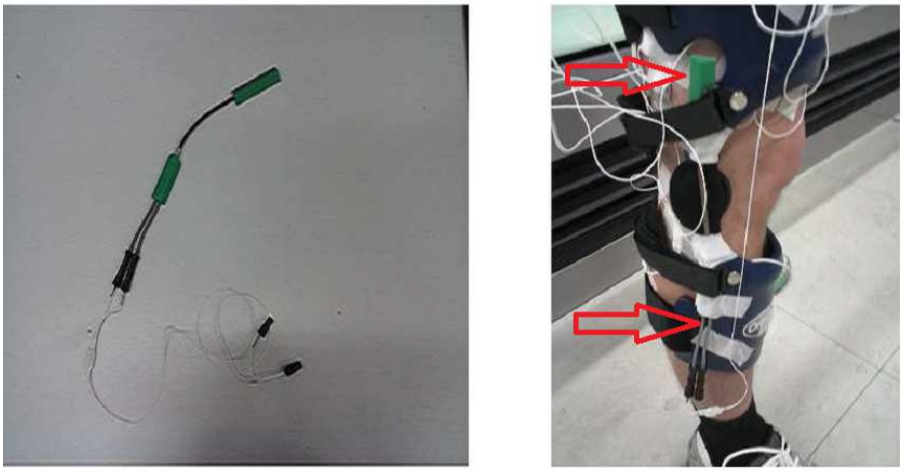

Figure 3.4: Goniometer and the device attached to the orthosis

3.2.2.3 ACC

The knee joint is basically made up of four bones: the largest thigh bone, **femur**, is attached by ligaments and capsule to the **tibia**; the **fibula**, that is located next to the tibia and runs parallel to it and, the **patella** (or knee cap), that moves along with the knee. Figure 3.5 shows knee's bone structure.

Figure 3.5: Principal bones of the knee joint [8]

The movements of the knee involve directly the femur and the tibia that are recruited by muscular contraction and tendon response. We used one triaxial accelerometer for each bone. Considering the accelerometers location, we put them vertically aligned with the patella, with the positive y axis pointing to the floor, placed on the frontside of the orthosis, one on the lower part and other on the upper part to measure the acceleration of the tibia and the femur respectively (Figure 3.6).

Figure 3.6: Placement of the ACC sensors

3.2.2.4 Recording devices

To record the data from our subjects, we used two bioPLUXresearch connected by the synchronism toolkit.
The bioPLUXresearch (figure 3.7) is a device that collects and digitalizes signals from the sensors, transmitting them via bluetooth to the computer where the signals are shown in real-time. It has eight 12-bit analogue channels, with a sample frequency of $1000Hz$. It also has a digital port, a connector for the transformer to recharge the internal battery and a channel to connect the reference electrode, an essential requirement to correctly monitor the electromyographic signal.

Figure 3.7: bioPLUXresearch system

In total we used fourteen of the sixteen available channels for our recording procedure. However, since one of the goniometer channels does not provide relevant information, we deleted it; so, at the end, we resorted thirteen channels.

3.3 Acquisition Protocol

The signal acquisition protocol was performed by all of the subjects.
The acquisition protocol is composed by a set of 8 activities, described in the following items, where an activity is considered as a sequence of movements.

- **Activity 1. Walk and turn**: Each participant was asked to walk and turn to his left side several times performing 10 "squares" in total. We acquired one recording per subject;

- **Activity 2. Sit and stand**: The activity 2 consisted of one recording per subject where the participant, starting in a lower position, got up and sat down consecutively until 20 repetitions;
- **Activity 3. Sit, stand and walk a few steps**: Starting in a lower position, each participant was requested to get up and walk a few steps; here, five recordings per subjects were collected;
- **Activity 4. Walk to a chair, turn, sit and stand**: Each volunteer had to walk to a chair, turn, sit and stand consecutively until 20 repetitions. We also acquire one single recording per subject;
- **Activity 5. Walk and stairs up**: Each volunteer was asked to walk and walk stairs up a group of steps. In total, we collected ten recordings for each subject;
- **Activity 6. Walk and stairs down**: Each volunteer was asked to walk and walk stairs down a group of steps. In total, we collected ten recordings for each subject;
- **Activity 7. Ascend a hill**: We acquired two recordings of about two minutes each where each volunteer was requested to ascend a hill. The treadmill used as a 'hill' was positioned with 27% of inclination;
- **Activity 8. Descend a hill**: Similar to activity 7, here the participants descended a hill during approximately two minutes for each one of the two recordings. The treadmill used as a 'hill' was positioned with 27% of inclination.

These activities took place at the BioMotion Lab of the *KIT-Karlsruhe Institute of Technology Sports' Institute*.

4

Segmentation

In this chapter we intend to explain the segmentation procedure applied on the signals so that, at last, we can provide an overview about our *data corpus*. Therefore, we begin by presenting some of the signals resulting from the acquisition.

4.1 Signal's overview

In this section, we will exhibit an example of the raw data obtained directly from the acquisition.
As will be seen, each wave has its proper shape which can provide us different information about the motion in action.
Considering the EMG, it is important to refer that the instance when muscular activity occurs depends on the function that muscle has; e.g, when flexors muscles show some contraction, extensors muscles tend to be approximately at rest and vice-versa.
On the other hand, the ACC wave allow us to understand how and with which acceleration both lower limb's segments move.
The GON output show the evolution of knee's angular position over time.
All of the biosignals' acquisition procedure was accompanied by video recording to be used in future stages of this project.

As an example, the figures 4.1, 4.2 and 4.3 represent the EMG, GON and ACC signals acquired for the activity 5, *Walk and Walk stairs up*, respectively.

4.2 Segmentation

Our future classification is based on creating an one-cycle wave model for each class.

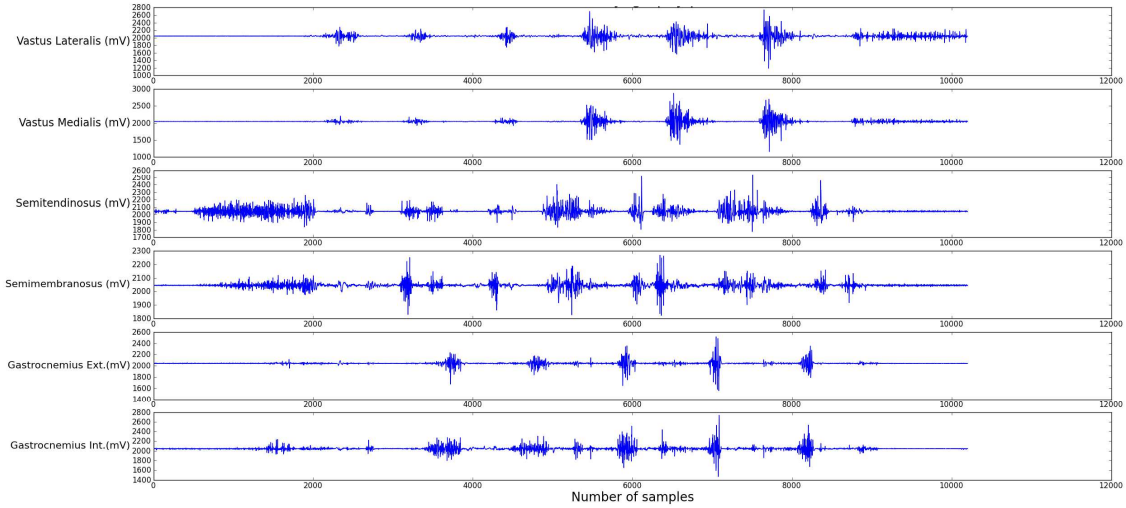

Figure 4.1: EMG raw signals for the sequence walk and walk stairs up. Plot shows quadriceps', hamstrings' and gastrocnemius' activity, from top to bottom

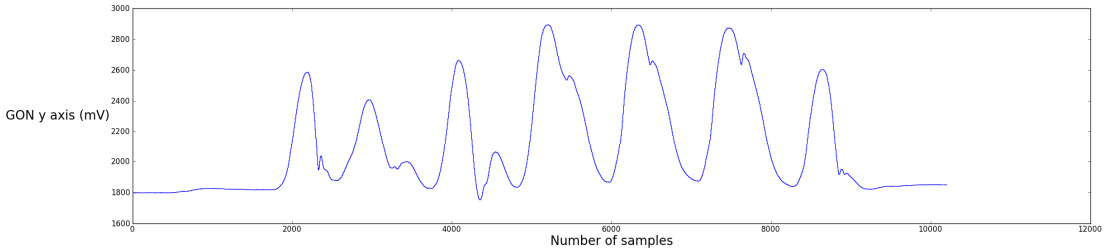

Figure 4.2: GON raw signal for the sequence walk and walk stairs up. Plot shows how the range of motion evolutes over time for the y axis

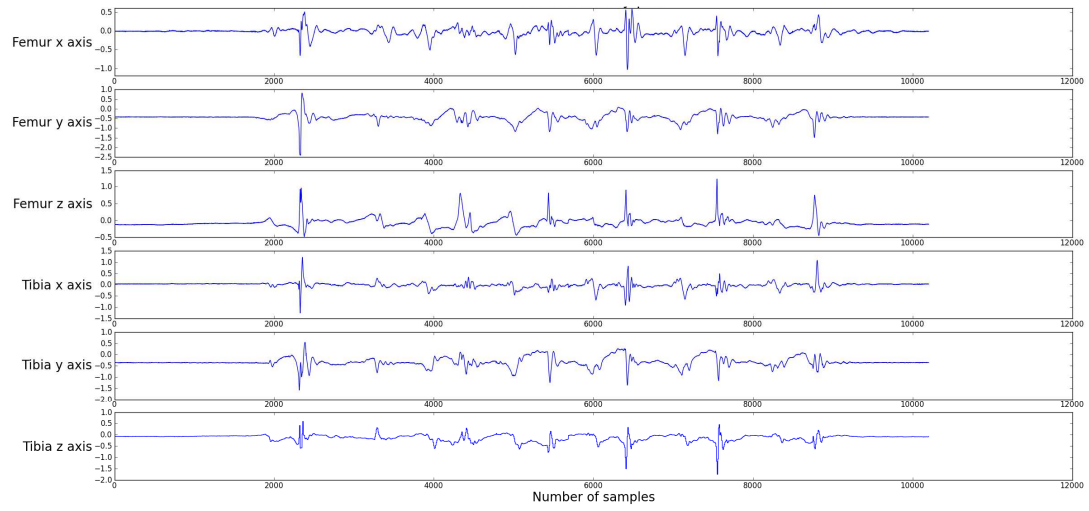

Figure 4.3: ACC raw signals for the sequence walk and walk stairs up. Plot shows femur's (x, y, x) and tibia's (x, y, z) acceleration, respectively, from top to bottom

The purpose of the data segmentation step is to split the continuous sensor recordings into motion primitives to be used as the classifier's input. For the periodic motions *walk*, *stairs up*, *stairs down*, and *ascend* and *descend* a hill, we define a motion primitive as one complete gait cycle. For motions like *stand-to-sit* and *sit-to-stand*, we define a motion primitive as the movement that occurs between the two static postures "stand" and "sit". We segment each continuous periodic signals in its unique motion primitives. We segment automatically the periodic activities according to the standard segmentation of gait cycles in [23, 39, 40].

A gait cycle consists of a stance and a swing phase and starts and ends with the initial contact of the heel on the floor. At this point of the gait cycle the knee angle is minimal. Our automatic segmentation algorithm computes the local minima of the goniometer signal and takes these as segment borders. The signal is then split into motion primitives according to the found segment borders. Figure 4.4 illustrates this procedure.
The non-periodic movements *stand-to-sit* and *sit-to-stand* are segmented manually.

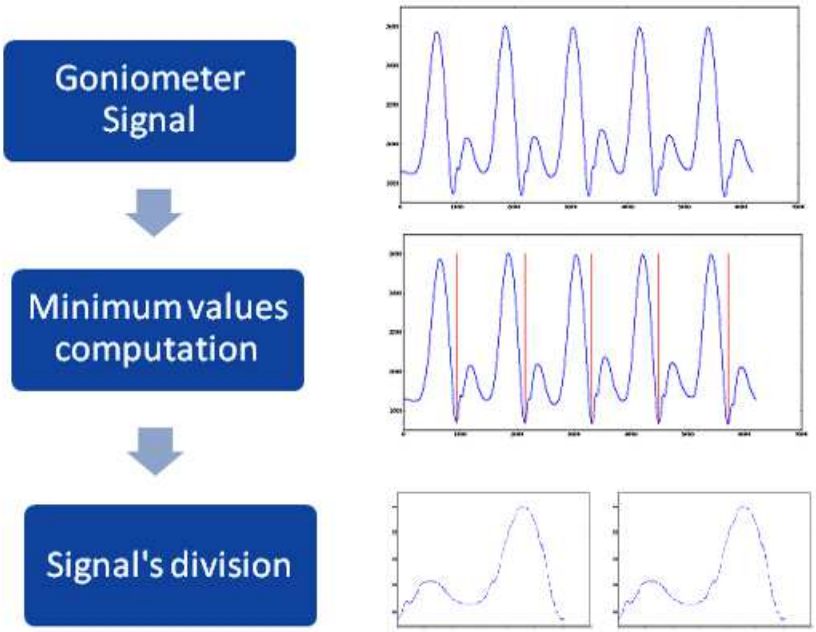

Figure 4.4: Representative scheme for the automatic segmentation algorithm. The signals refer to the movement *walk*

We additionally checked the results of the automatic segmentation manually to verify the correctness of our data segmentation.

The figures 4.5 and 4.6 show our segmentation results for the activity 5, previously shown.

4.2.1 Data Corpus

After acquisition and segmentation of all recorded data, we reached a total of 3858 isolated cycles for 7 movements: *walk*, *stand-to-sit*, *sit-to-stand*, *stairs up*, *stairs down*, *ascend*

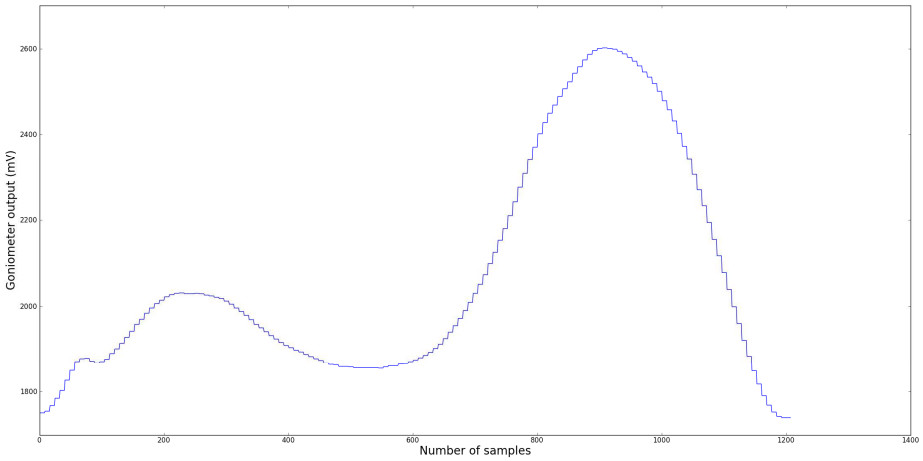

Figure 4.5: One cycle for walking based on the analysis of the goniometer output

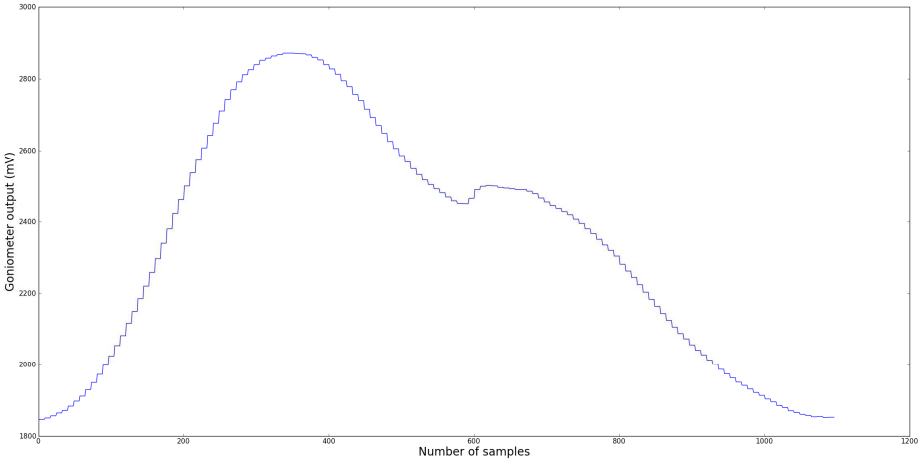

Figure 4.6: One cycle for walking stairs up based on the analysis of the goniometer output

and *descend*. Table 4.1 shows the original database's structure.

The database is unbalanced because the acquisition was not performed equally for each label. For example, for *ascend* and *descend*, we recorded two times 2min of walking which lead to a much higher number of cycles than the activities which were not performed on the treadmill, e.g. climbing stairs. Our classifier computes the *maximum a posteriori probability* which is a method used to obtain predictions on the most probables hypothesis. Hence, the classifier's input should have the same amount of information per each class. In order to get a balanced dataset for the evaluation we randomly chose 17 motion primitives per person for each activity, which is the minimum number of samples we recorded over all activities. The resulting balanced data corpus therefore consists of 714 motion primitives. Table 4.2 shows the operational database's structure.

These data were used as HMM's input for several experiments whose procedures and results are presented on chapter 6.

Movements	Number of isolated cycles
Walk	1356
Sit-to-stand	121
Stand-to-sit	116
Stairs up	170
Stairs down	172
Ascend	902
Descend	1021
Total	3858

Table 4.1: Number of isolated cycles from all subjects for each movement from all original acquired data

Movements	Number of isolated cycles
Walk	102
Sit-to-stand	102
Stand-to-sit	102
Stairs up	102
Stairs down	102
Ascend	102
Descend	102
Total	714

Table 4.2: Number of isolated cycles from all subjects for each movement randomly selected for a balanced database

5

Classification using Hidden-Markov-Models HMM

This chapter presents an overview about the HMM decoding used in this work. During the exposition, we will outline the differences between the standard HMM and the applied decoding procedure. Section 5.1 summarizes the classification procedure applied on this project.

5.1 Classification and Feature Extraction

We used continuous density HMM as classifier [20]. Since HMMs can model stochastic processes over time, they are well suited to model signals that have a characteristic temporal pattern, which is typically true for human motions. For each motion primitive we use an HMM with a left-to-right topology with 10 states and a Gaussian Mixture Model (GMM) with two components. We apply four iterations of Expectation Maximization (EM) training in each of the experiments. As aforementioned, we used the BioKit toolbox developed at the Cognitive Systems Lab for the training and decoding.

For feature extraction the signal is windowed using a rectangular window function with 50ms window length and no window overlap. All features are computed on the resulting windows. We denote the samples in one window by $(x_1, \ldots, x_N)$ where N is the total number of samples per window. Along the experiments, for each window, we extracted different combinations of the following features:

- *Average*

$$avg = \frac{1}{N} \sum_{k=0}^{N-1} x_k \tag{5.1}$$

- *Root mean square (RMS)*

$$RMS = \sqrt{\frac{x_1^2 + x_2^2 + \ldots + x_N^2}{N}} \tag{5.2}$$

We therefore get a one-dimensional feature vector for the goniometer signal and six-dimensional feature vectors for the six accelerometer channels as well as the six EMG channels. We use feature fusion, also known as early fusion, to fuse the different signal modalities. Depending on the signal type, the features are computed and then combined in one feature vector by concatenation. Feature fusion is an appropriate fusion scheme if the underlying processes that produce the signals are synchronized. This can be assumed in our case because the underlying process, moving the knee, is the same for all signal modalities. Additionally, since all modalities were recorded synchronous with the same sampling rate, we consider this fusion scheme to be a reasonable choice.

The experiments and results are presented and discussed on section 6.1.

5.2 BioKit

In this work, we used the *BioKit* toolbox which is a software from Cognitive Systems Lab that performs the HMM analysis.

Given a sequence of observations, the BioKit converts them into feature vectors and stores them in different data structures.

After the conversion, the HMM is initialized: definition of the number of states, number of gaussians, dimensionality and models' list. Each model (or *atom*) refers to the most primitive unit of which more complex models can be built; for example, in speech recognition, atoms are phonems. A *token* is created from atoms; for example, words (groups of letters). In this work, movements are the most basic unit we can get; so, tokens are atoms. Thus, each motion primitive is one atom which is described by one model. Considering this fact, it it possible to model arbitrary sequences of motion primitives.

The left-to-right HMM topology in use presents a mixture model defined.A mixture model is a way to represent the emission probability distribution. In this project, we used *GMM*. In other words, GMM is a combination of Normal distributions to model more complex distributions; the more components it has, the more complex distributions it can model.

According to a standard procedure, the Viterbi path would be computed for each model. However, if we work with a large space this calculation becomes complex and time consuming. Thus, the BioKit introduces the concept of *Beam Search* which deletes the less probables paths based on score and number of hypotheses' limitation. A *hypothesis* can

be seen as one possible path during the search. In short words, the beam search prune the hypothesis.

Furthermore, this software uses by default diagonal covariance matrices instead of full covariance matrices which decreases the number of parameters to train. GMMs are a combination of multidimensional normal distributions. A normal distribution is defined by mean and variance, and in the multidimensional case by the mean vector and the covariance matrix. To limit the number of parameters that need to be estimated, diagonal covariances matrices are used.

As an additional BioKit's feature, it is possible to define a *grammar* (possible sequences of atoms), which also helps on eliminating non-interesting paths.

On the next section we will present the experiments and its outcomes resulting from the recognizer built according to this toolbox.

6

Experiments

The goal of this chapter is lodge to the reader the experiments investigated and the results from our recognizer as well as their discussion (section 6.2).

6.1 Experiments and Results

The main goal of this project is to investigate how well movement primitives can be correctly recognized. Since we are working with three different types of signals, our intention is to evaluate how much the different signal's modalities contribute to the overall performance of the classifier. Hence, we explore all possible combinations of the different signals: EMG, GON, ACC, EMG&GON, GON&ACC, EMG&ACC and EMG&GON&ACC, whether in a context of subject's dependency or independency. After the extraction of the features referred in 5.1, in total, we work with 6, 1, 6, 7, 7, 12 and 13-dimensional features spaces, respectively. Each experiment was repeated four times.

For each different context, we compute the accuracy (see section 2.4) of the respective leave-one-out cross-validation (see section 2.4).

6.1.1 Experiment 1: Subject's dependent context

The first test procedure investigates how the recognizer performs in a subject's dependent context.
Subject's dependent context is when we train the recognizer only with files of one subject and test it with another data from the same subject.

Signals' Combination	Classification Accuracy (%)
EMG	65.41 ± 0.17
GON	83.33 ± 0.12
ACC	97.34 ± 0.01
EMG&GON	72.13 ± 0.17
GON&ACC	98.32 ± 0.05
EMG&ACC	81.23 ± 0.14
EMG&GON&ACC	87.54 ± 0.13

Table 6.1: Classification accuracy (mean and standard deviation) per combination of signals in a subject's dependent case

To evaluate the subject-dependent accuracy of the classifier we performed a leave-one-out cross-validation for each subjects data. We chose a set of 119 motion primitives available for each subject. Figure 6.1 and table 6.1 shows a breakdown of the results for each of the signals' combination.

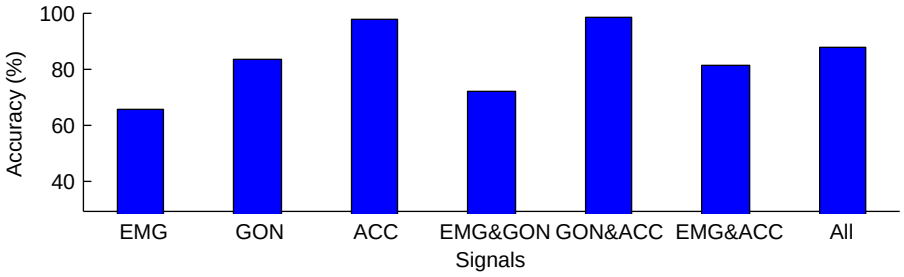

Figure 6.1: Classification accuracy per combination of signals in a subject's dependent case

Based on these results, the recognizer accomplished its task with an accuracy between 65 and 98% with an average accuracy of 84%. We can also conclude that the combination of GON&ACC presents the highest classification accuracy. Since these signals present a more defined shape and consequently, a more defined pattern, this result could be expected. Likewise, the EMG presents the lower accuracy.

The confusion matrices for each combination are represented on tables 6.2 to 6.8.

	Walk	**Stand-to-sit**	**Sit-to-stand**	**Stairs up**	**Stairs down**	**Ascend**	**Descend**
Walk	**26**	0	6	17	3	21	27
Stand-to-sit	1	**95**	4	0	0	0	0
Sit-to-stand	3	4	**90**	2	1	0	0
Stairs up	9	0	1	**46**	8	12	25
Stairs down	6	0	4	10	**53**	8	20
Ascend	3	0	8	8	2	**67**	13
Descend	7	0	0	6	2	5	**80**

Table 6.2: Confusion matrix for EMG set in a subject-dependent context (in percentage)

	Walk	Stand-to-sit	Sit-to-stand	Stairs up	Stairs down	Ascend	Descend
Walk	**89**	0	0	2	0	0	9
Stand-to-sit	0	**99**	0	0	1	0	0
Sit-to-stand	0	0	**96**	2	1	1	0
Stairs up	1	0	0	**73**	16	2	9
Stairs down	0	0	0	3	**92**	0	5
Ascend	14	0	0	9	2	**62**	14
Descend	8	0	0	0	18	2	**73**

Table 6.3: Confusion matrix for GON set in a subject-dependent context (in percentage)

	Walk	Stand-to-sit	Sit-to-stand	Stairs up	Stairs down	Ascend	Descend
Walk	**90**	0	0	3	6	0	1
Stand-to-sit	0	**100**	0	0	0	0	0
Sit-to-stand	0	0	**100**	0	0	0	0
Stairs up	0	0	0	**98**	0	0	2
Stairs down	0	0	0	1	**97**	0	2
Ascend	0	0	0	1	1	**98**	0
Descend	0	0	0	2	0	0	**98**

Table 6.4: Confusion matrix for ACC set in a subject-dependent context (in percentage)

	Walk	Stand-to-sit	Sit-to-stand	Stairs up	Stairs down	Ascend	Descend
Walk	**43**	0	0	8	9	16	25
Stand-to-sit	1	**98**	1	0	0	0	0
Sit-to-stand	1	1	**97**	0	1	0	0
Stairs up	5	0	0	**55**	6	10	25
Stairs down	3	10	1	0	**55**	10	22
Ascend	2	0	2	10	2	**74**	11
Descend	4	0	0	7	1	5	**83**

Table 6.5: Confusion matrix for EMG&GON set in a subject-dependent context (in percentage)

	Walk	Stand-to-sit	Sit-to-stand	Stairs up	Stairs down	Ascend	Descend
Walk	**95**	0	0	0	3	1	1
Stand-to-sit	0	**100**	0	0	0	0	0
Sit-to-stand	0	1	**99**	0	0	0	0
Stairs up	0	0	0	**98**	2	0	0
Stairs down	0	0	0	0	**98**	0	2
Ascend	0	0	0	1	0	**99**	0
Descend	0	0	0	0	1	0	**99**

Table 6.6: Confusion matrix for GON&ACC set in a subject-dependent context (in percentage)

	Walk	Stand-to-sit	Sit-to-stand	Stairs up	Stairs down	Ascend	Descend
Walk	**56**	0	0	15	5	10	15
Stand-to-sit	1	**98**	0	0	1	0	0
Sit-to-stand	2	1	**94**	2	1	0	0
Stairs up	2	0	0	**77**	6	11	4
Stairs down	7	0	0	3	**75**	2	13
Ascend	6	0	0	10	1	**82**	2
Descend	7	0	0	1	4	2	**86**

Table 6.7: Confusion matrix for EMG&ACC set in a subject-dependent context (in percentage)

	Walk	Stand-to-sit	Sit-to-stand	Stairs up	Stairs down	Ascend	Descend
Walk	**75**	0	0	8	7	3	7
Stand-to-sit	1	**98**	1	0	0	0	0
Sit-to-stand	1	1	**95**	2	1	0	0
Stairs up	2	0	0	**83**	7	8	0
Stairs down	2	0	0	5	**82**	1	10
Ascend	3	0	0	7	1	**89**	0
Descend	7	0	0	0	2	2	**89**

Table 6.8: Confusion matrix for EMG&GON&ACC set in a subject-dependent context (in percentage)

Each confusion matrix present how well the classifier performed in each activity type. Concerning the worst classified set, by analysing the table 6.2, we may infer that only 26% from all of the *walk* primitives are recognized correctly; 27% is labelled as *descend*, 21% as *ascend*, 17% as *stairs up*, 6% as *sit-to-stand* and the remaining 3% as *stairs down*. Additionally, for the best performing combination (table 6.6), we achieve high classification accuracies for all classes. As a further analysis, figure 6.2 and table 6.9 shows the classification accuracy per subject for the best performing combination.

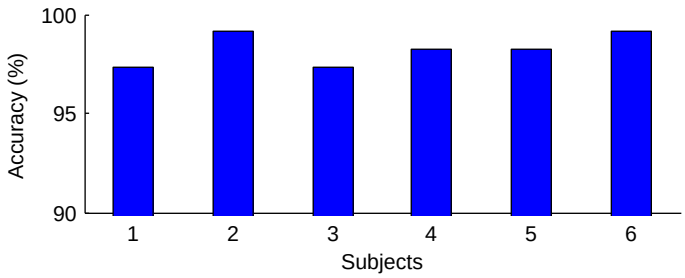

Figure 6.2: Classification accuracy per subjects for GON&ACC set in a subject's dependent case

High accuracies were reached for all subjects. Our system labelled the primitives with an accuracy between 97% and 99% with an average of 98%. For the subject dependent context, we believe a robust recognition is possible.

Subjects	Classification Accuracy (%)
1	97.32 ± 0.04
2	99.11 ± 0.02
3	97.32 ± 0.04
4	98.22 ± 0.03
5	98.22 ± 0.03
6	99.11 ± 0.04

Table 6.9: Classification accuracy (mean and standard deviation) per subject for GON&ACC set in a subject's dependent case

Signals' Combination	Classification Accuracy (%)
EMG	44.57 ± 13.87
GON	61.46 ± 11.67
ACC	75.05 ± 22.65
EMG&GON	47.94 ± 14.60
GON&ACC	78.70 ± 21.64
EMG&ACC	55.52 ± 14.46
EMG&GON&ACC	63.66 ± 17.14

Table 6.10: Classification accuracy (mean and standard deviation) per combination of signals in a subject's independent case

6.1.2 Experiment 2: Subject's independent context

The second test procedure investigates how the recognizer performs in a subject's independent context.
Subject's independent context is when we train the recognizer with a database formed by data of all subjects except the one we intend to evaluate and test only with data of that test subject.
We evaluate the subject-independent performance with a leave-one-out cross-validation on the subjects. We use all samples in our database, resulting in 595 samples for training and 119 samples for testing for each subject. Figure 6.3 and table 6.10 presents the results for each of the signal's combination.

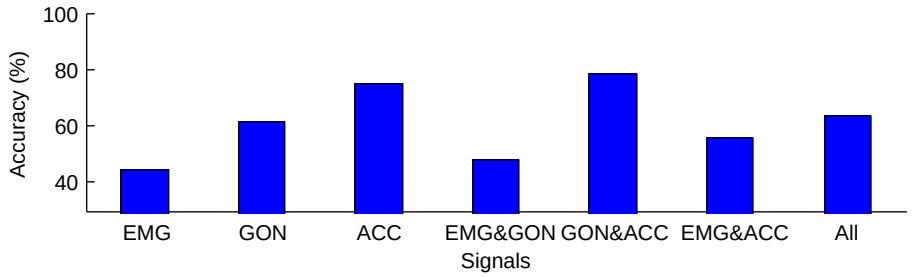

Figure 6.3: Classification accuracy per combination of signals in a subject's independent case

The recognizer performed with an accuracy between 44% and 79% with an average accuracy of 61%. We can also conclude that the combination GON&ACC exhibits the highest accuracy value, analogously to 6.1.1. However, we can state that, compared to the subject-dependent case, the accuracy is much lower which can be explained by the variations in human motion for different subjects.

The confusion matrices for each signal's combination are presented on tables 6.11 to 6.17.

	Walk	**Stand-to-sit**	**Sit-to-stand**	**Stairs up**	**Stairs down**	**Ascend**	**Descend**
Walk	**5**	0	2	31	6	50	7
Stand-to-sit	0	**80**	20	0	0	0	0
Sit-to-stand	0	19	**57**	0	3	19	3
Stairs up	1	0	1	**41**	21	10	26
Stairs down	0	0	5	15	**50**	17	13
Ascend	0	0	4	9	0	**76**	11
Descend	0	0	0	28	23	46	**3**

Table 6.11: Confusion matrix for EMG set in a subject-independent context (in percentage)

	Walk	**Stand-to-sit**	**Sit-to-stand**	**Stairs up**	**Stairs down**	**Ascend**	**Descend**
Walk	**36**	0	0	14	44	7	0
Stand-to-sit	0	**98**	2	0	0	0	0
Sit-to-stand	0	0	**71**	29	0	0	0
Stairs up	0	0	0	**66**	11	16	7
Stairs down	1	0	0	1	**86**	3	9
Ascend	2	0	0	6	10	**72**	11
Descend	1	0	0	0	79	17	**3**

Table 6.12: Confusion matrix for GON set in a subject-independent context (in percentage)

	Walk	**Stand-to-sit**	**Sit-to-stand**	**Stairs up**	**Stairs down**	**Ascend**	**Descend**
Walk	**74**	0	0	1	0	3	22
Stand-to-sit	0	**83**	0	3	0	0	14
Sit-to-stand	12	0	**83**	1	0	0	4
Stairs up	1	0	0	**90**	2	5	2
Stairs down	2	0	0	13	**56**	5	23
Ascend	28	0	0	5	0	**67**	0
Descend	17	0	0	0	14	0	**70**

Table 6.13: Confusion matrix for ACC set in a subject-independent context (in percentage)

For the worst performing combination (table 6.11), the movement *descend* is easily confused. From all of its primitives, only 3% are correctly recognized; 46% of them is labelled as *ascend*, 28% as *stairs up* and 23% as *stairs down*. Concerning the GON&ACC set, the classes *stairs down* and *ascend* are those with higher percentage of misclassification being confused with *descend* and *stairs up*, respectively. This is not surprising since the performed motions are very similar for these pair of activities.

	Walk	Stand-to-sit	Sit-to-stand	Stairs up	Stairs down	Ascend	Descend
Walk	**14**	0	7	14	8	48	10
Stand-to-sit	0	**80**	20	0	0	0	0
Sit-to-stand	0	10	**66**	0	9	5	11
Stairs up	0	0	1	**52**	17	25	5
Stairs down	0	0	5	16	**48**	14	17
Ascend	1	0	5	12	0	**70**	13
Descend	7	0	0	12	29	46	**6**

Table 6.14: Confusion matrix for EMG&GON set in a subject-independent context (in percentage)

	Walk	Stand-to-sit	Sit-to-stand	Stairs up	Stairs down	Ascend	Descend
Walk	**89**	0	0	0	4	0	7
Stand-to-sit	0	**83**	0	0	17	0	0
Sit-to-stand	0	0	**83**	17	0	0	0
Stairs up	0	0	0	**92**	4	4	0
Stairs down	4	1	1	9	**66**	1	18
Ascend	1	0	0	32	0	**67**	0
Descend	19	0	0	0	9	0	**72**

Table 6.15: Confusion matrix for GON&ACC set in a subject-independent context (in percentage)

	Walk	Stand-to-sit	Sit-to-stand	Stairs up	Stairs down	Ascend	Descend
Walk	**39**	0	6	22	6	25	3
Stand-to-sit	0	**89**	0	0	11	0	0
Sit-to-stand	10	4	**74**	4	0	7	2
Stairs up	4	0	0	**61**	11	24	0
Stairs down	4	0	4	14	**52**	12	14
Ascend	17	0	3	16	0	**57**	8
Descend	29	0	0	6	28	19	**18**

Table 6.16: Confusion matrix for EMG&ACC set in a subject-independent context (in percentage)

	Walk	Stand-to-sit	Sit-to-stand	Stairs up	Stairs down	Ascend	Descend
Walk	**60**	0	5	14	7	9	5
Stand-to-sit	0	**88**	0	0	12	0	0
Sit-to-stand	0	1	**77**	6	0	16	0
Stairs up	1	0	0	**66**	11	23	0
Stairs down	4	0	0	13	**55**	13	15
Ascend	13	0	0	19	4	**65**	0
Descend	20	0	0	2	22	18	**38**

Table 6.17: Confusion matrix for EMG&GON&ACC set in a subject-independent context (in percentage)

Subjects	Classification Accuracy (%)
1	36.13 ± 21.43
2	83.19 ± 10.11
3	89.08 ± 4.56
4	78.15 ± 8.17
5	94.12 ± 0.15
6	91.52 ± 0.87

Table 6.18: Classification accuracy (mean and standard deviation) per subject for GON&ACC set in a subject's independent case

Figure 6.4 and table 6.18 present the outcomes per subject for the best performing combination.

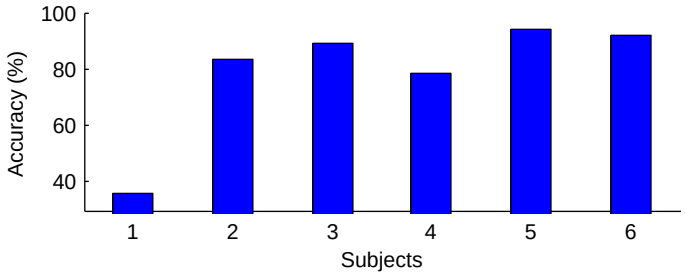

Figure 6.4: Classification accuracy per subjects for GON&ACC in a subject's independent case

Concerning the evaluation per subject, the recognizer performed with an accuracy between 36% and 94% with an average accuracy of 79%. Due to the small number of subjects, the generalization ability of the classifier is relatively low and, thus, we can see a low performance for subject 1. In order to support the results for subject 1, we can add that this subject, although healthy, has a proper way and unusual style of moving.

6.2 Discussion

This chapter comes in sequence of testing the performance of our recognizer, investigating the possibility to classify isolated human activities from biosignal sensors integrated into a knee orthosis. The system was evaluated on the task to discriminate seven different movements: *walk*, *stand-to-sit*, *sit-to-stand*, *stairs up*, *stairs down*, *ascend* and *descend*, leading to different classification accuracies depending on the signals' combination in study and/or context.

In 6.1.1, from all possible biosignals' modalities, we reached an average person-dependent accuracy of 84%. This outcome can be justified by the activities' low classification percentage in noisy signals such as EMG. Therefore, the EMG is not the right modality for this task. On the other hand, movements from well defined signals were expected to be

more correctly identified, which is the case of the GON&ACC group. Here, we achieved an average classification accuracy per subject of 98%.

The outcomes from experiment 1 lead us to conclude that is possible to accomplish a strong subject-dependent recognition.

In 6.1.2, for the different combination of signals, we reached an average person-independent accuracy of 61%. When compared to the subject's dependent case, the accuracy is lower which is explained by the inherent character of motion. The way of motion is an idiosyncratic feature determined by individual's weight, limb length, footwear and posture combined with kinematic characteristics. Likewise in 6.1.1, the combination of GON&ACC pointed out as having the highest correct identification of primitives, where the average classification accuracy per subject is 79%.

It is important to emphasize that, due to the small number of subjects, the overall recognition competence can not be guarantee.

Additionally, as a general conclusion, the movements *stairs down* and *ascend* are frequently confused with *descend* and *stairs up*, respectively, which is explained by the similarity of the performed motions.

Lastly, since orthosis are individual products, the outcome from experiment 1 is the most relevant result.

7

Conclusions and Further Work

In this chapter, we present a summary of our work as well as overall results and further work. Furthermore, the contributions to this project will be highlighted.

7.1 Conclusions

In this thesis we intended to investigate how well human isolated motions were correctly recognized based on different signals' combinations.

As we proposed, our project was divided into several stages previously discussed: *Acquisition*, *Signal processing and Segmentation* and *Classification*. The last part involves feature extraction and classification with HMM.

In the first part, *Acquisition*, we presented our database collecting procedure by recording several activities according to an acquisition protocol, using a setup of three different modalities of signals: EMG, GON and ACC. All of the sensors were positioned so we could measure the leg motion and the muscle activity of the wearer.

Trippingly, at *Signal processing and Segmentation*, we divided each continuous signal into several motion primitives semi-automatically. We reached a total of 3858 isolated primitive movements from which we used 714 as classifier's input, encompassing seven different motions: *walk*, *stand-to-sit*, *sit-to-stand*, *stairs up*, *stairs down*, *ascend* and *descend*.

At the last stage, *Classification*, after feature extraction, we applied a left-to-right topology HMMs with 2-dimensional GMM to classify these isolated cycles.

Figure 7.1 presents an overview diagram of our work.

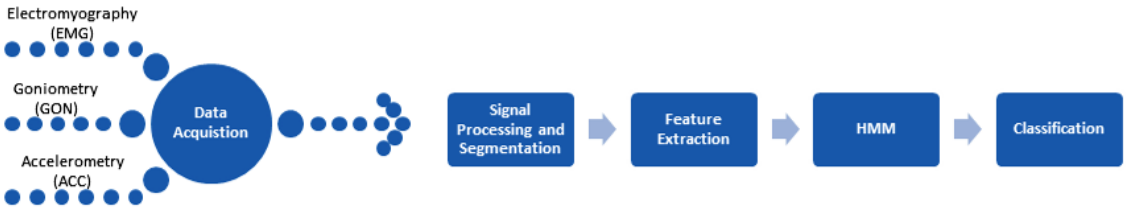

Figure 7.1: Work stages' diagram

In this work we evaluated the possibility to recognize human activities from different biosignal sensors attached to a knee orthosis or the skin under the orthosis. We investigated all possible signal modality combinations and found that the combination of GON&ACC gives the highest accuracy whether in a subject's dependent or independent context, with 98% and 79%, respectively. Based on background results' analysis, we can add that the recognizer frequently confuses the movements *stairs down* with *descend* and *ascend* with *stairs up*.

Along the work development, two papers [41,42] were published which are exposed on *Appendix* 8.

The core of this project was mainly developed at *CSL-Cognitive Systems Lab* at *Karlsruhe Institute of Technology* (Germany). The remaining tasks were ripened at *PLUX-Wireless Biosignals* in the context of its Research and Development (R&D) department. The excellency of professionals, good environment and facilities led to a strong work ethic and ended up to be an important and extremely enriching experience.

7.2 Further Work

The research project discussed presents some next future steps towards an active intelligent knee orthosis which we would like to probe lately. They are lodged next.

Recognition of continuous sequences of movements: In this research only isolated motions were identified. However, human motion is sequential whereby classification of different possible sequences of the same discriminated movements would be viable. For example, activities such as *stairs up, walk* or *sit, stand and walk* would be practicable to recognize. Additionally, this task could require video segmentation.

Recognizer's ability generalization: In order to have a more consistent conclusions and be possible to assertively generalize them, we should increase our database. Thus, the acquisition protocol could be performed by a higher number of healthy subjects.

Activity recognition is a widely studied field, possible to be applied in medicine, sports or research. Human activity recognition by biosignals' processing is a promising area to be explored specially because it can provide medical informations which can

be used as a pattern for further treatments or even diagnoses.

In the context of our project, the development of an active intelligent knee orthosis will enable the improvement of the wearer's quality of life, leading to a permanent use of the equipment which is the central issue to solve so a treatment procedure can succeed.

This research was a challenging, interesting, rewarding and enriching experience.

Bibliography

[1] R.C. Evans. *Illustrated orthopedic physical assessment*. Mosby/Elsevier, 2001.

[2] Flexors muscles. http://www.fitstep.com/Advanced/Anatomy/Quadriceps.htm. Accessed: 15/3/2012.

[3] Extensors muscles. http://www.iemily.com/article-830.html. Accessed: 15/3/2012.

[4] Gonarthrosis. http://nilseuropa.com/arthritis-knee-x-ray. Accessed: 30/3/2012.

[5] N. Nunes. *Algorithms for Time Series Clustering Applied to Biomedical Signals*. PhD thesis, Dissertação de Mestrado, Universidade Nova de Lisboa, Lisboa, 2011.

[6] N. Nunes, T. Araújo, and H. Gamboa. Two-modes cyclic biosignal clustering based on time series analysis.

[7] Hidden markov models. http://www.gta.ufrj.br/grad/07_2/viviane/HiddenMarkovModels-HMMs.html. Accessed: 18/08/2012.

[8] Knee bones. http://www.aclsolutions.com/anatomy.php. Accessed: 27/7/2012.

[9] E. MIRANDA. *BASES DE ANATOMIA E CINESIOLOGIA*. SPRINT.

[10] A.C. Guyton and J.E. Hall. *Textbook of medical physiology*, volume 9. Saunders Philadelphia, PA, 1991.

[11] J.D. Enderle and J.D. Bronzino. *Introduction to biomedical engineering*. Academic Pr, 2011.

[12] J.D. Bronzino. *The biomedical engineering handbook*, volume 2. CRC Pr I Llc, 2000.

[13] W. Norkin. Measurement of joint motion: A guide to goniometry (measurement of joint motion: A gde to goniometry) autho. 2009.

[14] R.W DeVaul and S. Dunn. Real-time motion classification for wearable computing applications.

[15] C. Amma, D. Gehrig, and T. Schultz. Airwriting recognition using wearable motion sensors. In *Proceedings of the 1st Augmented Human International Conference*, page 10. ACM, 2010.

[16] F. Foerster and J. Fahrenberg. Motion pattern and posture:correctly assessed by calibrated accelerometers.

[17] EJ Ciaccio, SM Dunn, and M. Akay. Biosignal pattern recognition and interpretation systems. *Engineering in Medicine and Biology Magazine, IEEE*, 12(3):89–95, 1993.

[18] SB Kotsiantis, ID Zaharakis, and PE Pintelas. Supervised machine learning: A review of classification techniques. *FRONTIERS IN ARTIFICIAL INTELLIGENCE AND APPLICATIONS*, 160:3, 2007.

[19] I.H. Witten, E. Frank, and M.A. Hall. *Data Mining: Practical machine learning tools and techniques*. Morgan Kaufmann, 2011.

[20] L.R. Rabiner. A tutorial on hidden markov models and selected applications in speech recognition. *Proceedings of the IEEE*, 77(2):257–286, 1989.

[21] I. Boesnach, J. Moldenhauer, C. Burgmer, T. Beth, V. Wank, and K. Bos. Classification of phases in human motions by neural networks and hidden markov models. In *Cybernetics and Intelligent Systems, 2004 IEEE Conference on*, volume 2, pages 976–981. IEEE, 2004.

[22] K. Luttgens and N. Hamilton. *Kinesiology:Scientific Basis of Human Motion, 9th Ed.* Madison,WI: Brown and Benchmark, 1997.

[23] D.H. Sutherland. The evolution of clinical gait analysis: Part ii kinematics. *Gait & posture*, 16(2):159–179, 2002.

[24] M.W. Whittle. *Gait analysis: an introduction*. 2003.

[25] A. Duhamel, JL Bourriez, P. Devos, P. Krystkowiak, A. Destee, P. Derambure, and L. Defebvre. Statistical tools for clinical gait analysis. *Gait & posture*, 20(2):204–212, 2004.

[26] R. Takeda, S. Tadano, M. Todoh, M. Morikawa, M. Nakayasu, and S. Yoshinari. Gait analysis using gravitational acceleration measured by wearable sensors. *Journal of biomechanics*, 42(3):223–233, 2009.

[27] F. Foerster, M. Smeja, and J. Fahrenberg. Detection of posture and motion by accelerometry: a validation study in ambulatory monitoring. *Computers in Human Behavior*, 15(5):571–583, 1999.

[28] R. Moe-Nilssen and J.L. Helbostad. Estimation of gait cycle characteristics by trunk accelerometry. *Journal of biomechanics*, 37(1):121–126, 2004.

[29] MJ Mathie, A.C.F. Coster, NH Lovell, and BG Celler. Detection of daily physical activities using a triaxial accelerometer. *Medical and Biological Engineering and Computing*, 41(3):296–301, 2003.

[30] G. Welk and J. Differding. The utility of the digi-walker step counter ro assess daily physical activity patterns. *Medicine and Science in Sports and Exercise*, 9(32):481–488, 2000.

[31] D.C. Preston and B. Ellen. *Electromyography and neuromuscular disorders*. Elsevier Butterworth-Heinemann, 2005.

[32] R.H.T. Edwards. Human muscle function and fatigue. In *Ciba Foundation Symposium 82-Human Muscle Fatigue: Physiological Mechanisms*, pages 1–18. Wiley Online Library, 1981.

[33] V.T. Inman, HJ Ralston, JB De CM Saunders, MB Bertram Feinstein, and E.W. Wright Jr. Relation of human electromyogram to muscular tension. *Electroencephalography and clinical Neurophysiology*, 4(2):187–194, 1952.

[34] D.G. Lloyd and T.F. Besier. An emg-driven musculoskeletal model to estimate muscle forces and knee joint moments in vivo. *Journal of biomechanics*, 36(6):765–776, 2003.

[35] PJ Rowe, CM Myles, C. Walker, and R. Nutton. Knee joint kinematics in gait and other functional activities measured using flexible electrogoniometry: how much knee motion is sufficient for normal daily life? *Gait & posture*, 12(2):143–155, 2000.

[36] E.Y. Suda. Análise eletromiográfica comparativa de tornozelo durante a aterrissagem em jogadores de vôlei com instabilidade crônica. 2011.

[37] C. Fleischer, C. Reinicke, and G. Hommel. Predicting the intended motion with emg signals for an exoskeleton orthosis controller. In *Intelligent Robots and Systems, 2005.(IROS 2005). 2005 IEEE/RSJ International Conference on*, pages 2029–2034. IEEE, 2005.

[38] C. Amma, M. Georgi, and T. Schultz. Airwriting: Hands-free mobile text input by spotting and continuous recognition of 3d-space handwriting with inertial sensors. In *Wearable Computers (ISWC), 2012 16th International Symposium on*, pages 52–59. IEEE, 2012.

[39] S.J. Farquhar, K.R. Kaufman, and L. Snyder-Mackler. Sit-to-stand 3 months after unilateral total knee arthroplasty: Comparison of self-selected and constrained conditions. *Gait & posture*, 30(2):187–191, 2009.

[40] KJ Deluzio and JL Astephen. Biomechanical features of gait waveform data associated with knee osteoarthritis: an application of principal component analysis. *Gait & posture*, 25(1):86–93, 2007.

[41] D. Rebelo, C. Amma, H. Gamboa, and T. Schultz. Human activity recognition for an intelligent knee orthosis. *6th International Joint Conference on Biomedical Engineering Systems and Technologies*, 2013.

[42] N. Nunes, D. Rebelo, R. Abreu, H. Gamboa, and A. Fred. *Clustering Algorithm for Human Behaviour Recognition based on Biosignals Analysis*. 2012.

8

Appendix

In this appendix we present the papers written during the Master's Thesis period. The first paper consists on a chapter of the book *'Human Behavior Recognition Technologies: Intelligent Applications for Monitoring and Security'* and it is entitled *'Clustering Algorithm for Human Behavior Recognition based on Biosignals Analysis'* [42]. The second paper is entitled *'Human Activity Recognition for an Intelligent Knee Orthosis'* and it was submitted and accepted to the *'6th International Joint Conference on Biomedical Engineering Systems and Technologies'* (BIOSTEC 2013), at BIOSIGNALS 2013, which will take place in Barcelona, on February 2013 [41].

Clustering Algorithm for Human Behavior Recognition based on Biosignals Analysis

Neuza Nunes[1], Diliana Rebelo[2], Rodolfo Abreu[2], Hugo Gamboa[2], Ana Fred[3,4]

[1] PLUX - Wireless Biosignals S.A., 1050-059 Lisboa, Portugal
[2] CEFITEC, Physics Department, FCT-UNL, 2829-516 Caparica, Portugal
[3] Electrical and Computer Engineering Department, IST – UTL, 1049 - 001 Lisboa, Portugal
[4] Pattern and Image Analysis, Instituto de Telecomunicações, 1049 – 001, Lisboa, Portugal

ABSTRACT

Time series unsupervised clustering has shown to be accurate in various domains and there is an increased interest in time series clustering algorithms for human behavior recognition.
We have developed an algorithm for biosignals clustering, which captures the general morphology of signal's cycles in one mean wave. In this chapter we further validate and consolidate it and make a quantitative comparison with a state-of-the-art algorithm which uses distances between data's cepstral coefficients to cluster the same biosignals. We were able to successfully replicate the cepstral coefficients algorithm and the comparison showed that our mean wave approach is more accurate for the type of signals analyzed, having a 19% higher accuracy value. We also tested the mean wave algorithm with biosignals with three different activities in it, and achieved an accuracy of 96.9%. Finally, we performed a noise immunity test with a synthetic signal and noticed that the algorithm remained stable for signal-to-noise ratios higher than 2, only decreasing its accuracy with noise of amplitude equal to the signal.
The necessary validation tests performed in this study confirmed the high accuracy level of the developed clustering algorithm for biosignals which express human behavior.

INTRODUCTION

The constant chase for human well-being has led researchers to increasingly design new systems and applications for a continuous monitoring of patients through their biological signals. In the past, human activity tracking techniques focused mostly on observations of people and their behavior through a great amount of cameras. However, the use of wearable sensors has been increasingly sought because it allows continuous acquisitions in different locations, being independent from the infrastructures. The recognition of human behavior through wearable sensors has a vast applicability. In the sports field, for example, there is a need for wearable sensors to assess physiological signals and body kinematics during free exercise. Wearable sensors have also major utility in healthcare, particularly for monitoring elderly and chronically ill patients in their homes, through Ambient Assisted Living (AAL).

Human body has always been considered a complex machine in which all parts work harmoniously. Nevertheless, the endless pursuit for the optimal human performance has become an important work area of digital signal processing. Therefore, monitoring athletes is the logical way to achieve the best patterns that can be compared to pathological signals in order to contribute for patient's rehabilitation. Thereby, the continuous monitoring and evaluation of athletic performance allow the coaches to establish an optimal training program. In addition, it is useful for non-professional athletes to establish and achieve their personal goals (R. Santos et al., 2012).

The main goal of AAL is to develop technologies which enable users to live independently for a longer period of time, increasing their autonomy and confidence in accomplishing some daily tasks (known as ADL - Activities of Daily Livings). However, AAL was also designed to reduce the escalating costs associated with health-care services in elderly people.
Thus, AAL's systems are used to classify a large variety of situations such as falls, physical immobility, study of human behavior and others. These systems are developed using a Ubiquitous Computing approach (AAL4ALL Project, 2012) (where sensors and signals' processing are executed without interfering on ADL) and must monitor activities and vital signs in order to detect emergency situations or deviations from a normal medical pattern (G.N. Rodrigues et al., 2010). Ultimately, AAL solutions automate this monitoring by software capable of detecting those deviations.

Signal-processing techniques have been developed to extract relevant information from biosignals which aren't easily detected in the raw data. However, most of these techniques are integrated in tools for specific biosignals, such as electrocardiography, respiration, accelerometry, among others. Thus, a single tool to recognize the morphology of the signal without prior information, analyzing and processing it accordingly is a recurrent necessity.
The smallest change in the signal's morphology over time may contain information of the utmost importance; hence, the detection of those changes has received much attention in this field. The recognition of different patterns in the signal's morphology is usually based on clustering or classification approaches. The ultimate goal is a generic and automatic classification system that doesn't require prior information and produces an efficient analysis whichever the type of the signal used.

In the following sections we summarize the scope and results of the developed algorithm and further evaluate it by testing it in a variety of contexts and validating it with a state-of-the art approach for time-series clustering.

RELATED WORK

N. Nunes (2012) presented an advanced signal processing algorithm for pattern recognition and clustering purposes applied to time varying signals collected from the human body. The recognition of differences in the signal's morphology produced by physiological abnormalities (arrhythmia, for example) or different conditions of the subject's state (walking or running, for example) was tested by collecting a set of cyclic biosignals with two distinctive modes. The acquired signals were the input of the generic algorithm. This algorithm knows beforehand the number of modes the signal has and is the base function to identify the individual cycles in a signal. The result of this algorithm is a single wave, a mean wave which is an averaging of all signal cycles aligned in a notable point.
As we're working with cyclic signals, the first step of the mean wave algorithm is the detection of the signal's fundamental frequency. With the fundamental frequency value we could compute the sampling size of a signal's cycle, and with that window size value, we randomly select a part of the signal with the same number of samples as the window size. Then we slide the smaller window part of the signal through the original signal, one sample at a time, computing the distance of the two waves present in those windows. After going through all the original data, we have as result a signal composed with distance values. The minimum points of the distance signal will be our events.
With the events computed, we are able to cut the signal into periods that we assume as our signal cycles. This way, based on all cycles, we could estimate the mean value to each cycle sample, and compose a mean wave. A standard deviation error wave is computed with the same principle, calculating the standard deviation error instead of the mean value for each sample. After this, a final adjustment was made: the alignment of the signal's cycles. The position of the mean wave's minimum point (a notable point) was detected, and that become our trigger point. With this trigger point, the events were recalculated and used to compute a mean wave again, so the cycles are aligned and the resultant mean wave more accurate.

The algorithm then has a k-means clustering phase which uses the information gathered from the mean wave approach to separate the several modes of the original signal. As the implemented mean wave approach accurately identifies the morphology of a signal, it can be a powerful tool in several areas – as a clustering basis or for signal analysis. The algorithm produced is signal-independent with high level of abstraction, and therefore can be applied to any cyclic signal with no major changes in the fundamental frequency. This type of generic signal interpretation overcomes the problems of exhaustive, lengthy signal analysis and expert intervention highly used in the biosignal's classification field.

Several approaches for time series comparison have been proposed in literature. The most straightforward approach relies on similarity measures which directly compare observations or features extracted from raw data. Besides the measurements made directly between time series, distances can also be computed with models built from the raw data. By modeling the raw data with a stochastic model, similarities are detected in the dynamics of different time series.

Linear Predictive Coding (LPC) is one of the methods of model compression and is widely used in speech analysis. Linear prediction filters attempt to predict future values of the input signal based on past signals.
The process of clustering time series models is usually a three-step procedure. Firstly, each time series is represented by a dynamical model, which is estimated using the given data. Secondly, a distance between

the dynamical models is computed over all the models estimated in the first stage - this distance measure can be the same used to cluster data or features extracted from the data. And finally, a clustering or a classification mechanism is performed based on the distance metric defined (J. Boets et al., 2005). This general methodology has been applied previously in different application areas, by estimating similarity measures between the LPC coefficients (G. Antoniol, 2005; P. Souza, 1997). However, another method, which estimates the cepstral coefficients from the LPC model and computes the distance between those coefficients, has been widely used achieving state of the art results in this field (K. Kalpakis, 2001; M. Corduas, 2008; A. Savvides, 2008).

In this chapter we intend to further validate our algorithm, comparing its accuracy with the state-of-the-art cepstral coefficients algorithm, test the results with more than two different modes, and perform a noise immunity test.

CEPSTRAL COEFFICIENTS ALGORITHM

Some of the publications that use the cepstral coefficients algorithm as a clustering mechanism used the Euclidean Distance between the LPC Cepstrum of two time series as their dissimilarity measure. The time series used in those publications were retrieved from a public database of ECG signals (Physionet, 2012).

The cepstral coefficients algorithm was replicated in our research and applied to the same public database, to achieve the same results as the ones documented. Our implementation was compared with the results exposed by Anthony Bagnall (2004), which uses an Euclidean distance between the cepstral coefficients to cluster the signals with a k-means clustering procedure.

We tested our implementation on a public ECG dataset which will be described below. The implementation and testing of the algorithm with the public ECG dataset will also be detailed next.

ECG Dataset

The public dataset of ECG signals is divided into three groups (*i.e.* three different classes for as the ECG records were acquired from people with different heart conditions). The number of records for each group corresponds to the people who volunteered for the study.

Group 1: 22 signal records of people with malignant ventricular arrhythmia (*i.e*, ECG acquisitions with 22 different people composed this group);
Group 2: 13 signal records of healthy people;
Group 3: 35 signal records of people with supraventricular arrhythmia.

Each signal record comprises 2 seconds of acquisition.

Figure 1. Examples of one signal record from each group from the public ECG dataset: a) malignant ventricular arrhythmia; b) normal ECG; c) supraventricular arrhythmia.

Figure 1 shows one arbitrary example of a signal record from each group. Two collections were defined in these studies: Collection 1 comprises the first two groups (35 signals), and Collection 2 gathers group 2 and 3 (48 signals). The cepstral coefficients algorithm received as input both collections to find two different clusters in each – representing the signals belonging to two different groups in each collection.

Implementation

Figure 2. Schematics for the cepstral coefficients algorithm implementation.

The first step of this algorithm is to fit a LPC model to the raw data, with a defined order. Among the direct transformations of LPC parameters, one is a filtering process to get the cepstral coefficients. We performed these steps using Python with the numpy and scikits talkbox packages.
Using the LPC coefficients estimation we computed the five cepstral coefficients (order - 1) of each time series. After that, the Euclidean distance between the signals' coefficients was estimated. Using equation 1 for all signals, a distances matrix is computed.

$$distance = \sqrt{\sum_{i=1}^{order-1} (sig_1 cc_i - sig_2 cc_i)^2} \qquad (1)$$

Being $sig_1 cc_i$ and $sig_2 cc_i$ the *i*cepstral coefficient from the first and the second signal, respectively. Finally, by retrieving the distance values and introducing that matrix into a K-Means algorithm, the time series are separated into different clusters.

With this implementation, the cepstral coefficients algorithm was successfully replicated, achieving the same results as described by Anthony Bagnall with the ECG dataset.

RESULTS

Comparison with cepstral coefficients algorithm

For the actual comparison between the performance of our mean wave algorithm and the cepstral coefficients algorithm, the dataset used was the one described in our previous publication – for which the activities performed and the final clustering results are exposed in Table 1. This table presents the number of cycles that composed the classification set for each task, the number of cycles that were correctly clustered, the errors and misses. The errors comprise misclassifications (i.e. samples that were attributed to different classes than expected) and misses comprise samples which weren't classified at all (this happened especially to the cycles which represent the transition between activities).

Table 1. Clustering results of the mean wave algorithm. From N. Nunes et al. (2012).

Task	*Number of Cycles*	*Cycles correctly clustered*	*Errors*	*Misses*
Synthetic	50	49	0	1
Walk and run	343	342	1	0
Run and jump	296	295	1	0
Jumps	85	84	1	0
Skiing	42	41	0	1
Elevation and squat	23	23	0	0
BVP rest and after exercise	165	159	4	2
All	1004	992	7	5

In the context tasks and signal types acquired, the accuracy was 99.3% for the separation of two different modes.

Table 2 gathers the clustering accuracy results obtained for each task and algorithms used (our mean wave algorithm and the cepstral coefficients algorithm). The accuracy percentage was computed using equation 2.

$$accuracy = \frac{Cycles_{cc}}{Cycles_N} \times 100\% \qquad (2)$$

Being $Cycles_{CC}$ the number of correctly clustered cycles and $Cycles_N$ the total number of cycles.

Table 2. Comparison of the results obtained with the cepstral coefficients and the mean wave algorithm.

Task	*Accuracy of cepstral coefficient algorithm*	*Accuracy of mean wave algorithm*
Synthetic	100.0%	100.0%
Walk and run	92.4%	99.7%
Run and jump	68.2%	99.7%
Jumps	82.1%	98.8%
Skiing	90.2%	100.0%
Elevation and squat	56.5%	100.0%
BVP rest and after exercise	68.7%	96.4%
Total	80.0%	99.3%

Our mean wave procedure presents a higher accuracy level for every signal but the synthetic waves, for which the accuracy is the same. Looking at the overall results, our algorithm achieved 99.3% accuracy, and the cepstral coefficients algorithm only 80.0% for the same signals - which from the tests with this database makes our approach a better option for clustering cyclic signals. To note also that our algorithm can be applied to a continuous signal with different modes in it, automatically separating the signal's cycles and computing a distance metric for each. The cepstral coefficients algorithm, however, has to be applied in separated signals - in this study we had to isolate the cycles before applying the cepstral coefficients procedure.

In conclusion, the comparison between the two algorithms confirmed that the mean wave algorithm has a high accuracy level, reaching better results, and is more suitable for the type of data analyzed than a state of the art algorithm in this area.

Validation

In this study we've also collected a new set of signals, with three different activities in each, composing over 2000 cycles.
To acquire the biosignals necessary for this study, we used a surface EMG sensor (*emgPLUX*) and a triaxial accelerometer (*xyzPLUX*). A wireless signal acquisition system, bioPLUX research (PLUX, 2012), was used for the signal's analogue to digital conversion and bluetooth transmission to the computer. This system has 12 bit ADC and a sampling frequency of 1000 Hz. In the acquisitions with the triaxial accelerometers, only the axis with inferior-superior direction was connected to the bioPLUX.

Several tasks were designed and executed in order to acquire signals with three distinct modes from 4 different subjects.

Before describing the activities executed in order to acquire the signals used for testing our algorithm, it is worthy to note that in all activities we used only the accelerometer's signal, except for activity 2 (walking, jumping, crouching), in which we tested also the EMG's signal.

Synthetic Signal:

To test our algorithm, a synthetic cycle was created using a low-pass filtered random walk (of 100 samples), with a moving average smoothing window of 10% of signal's length, and multiplying it by a *hanning* window. That cycle was repeated 296 times for the first mode, so all the cycles were identical. After a small break on the signal, the cycle was repeated 104 more times, but with an identical small change of 20 samples in all waves, creating a second mode. A third mode was created by changing the same 20 samples and repeating the new wave created 524 times. These three modes construct the synthetic wave represented in Figure 3.

Figure 3. Synthetic signal with three different modes (within each mode all waves are identical).

Activity 1 – Walking, Running, Walking, Jumping:

In this task, the accelerometer was located on the right hip along with the bioPLUX, so that the y axis's accelerometer was pointing downward. It was asked to the subjects to walk (for about 1 minute and half), run, walk again and jumpon the same place (each for about 1 minute). These four modes were executed non-stop. The signal acquired is demonstrated in Figure 4.

Figure 4. Activity 1: Walking, Running, Walking and Jumping.

Activity 2 – Walking, Jumping, Crouching:

With the accelerometer located on the right hip and oriented so that the y axis was pointing downward, the subjects performed a task of walking, vertical jumping and crouching, continuously. Each mode was executed 10 times and it is worthy referring that in walking mode, each step was considered a cycle. The signal acquired is demonstrated in Figure 5.

Figure 5. Activity 2 (ACC): Walking, Jumping and Crouching.

For the EMG's signal, electrodes were located on the ischiotibial of the right leg so that they were able to collect the muscle's activation signal during the activity. This signal was collected simultaneously with the accelerometer's signal. The signal acquired is demonstrated in Figure 6.

Figure 6. Activity 2 (EMG): Walking, Jumping and Crouching.

Activity 3 - Jumping, leg flexion and single leg vertical jumping

In this task, the following procedure was executed: normal vertical jumping, leg flexion and single leg vertical jumping. Each mode was repeated 10 times.
The subjects used an accelerometer located at the right hip and oriented so the y axis of the accelerometer was pointing downward. The signal acquired is represented in Figure 7.

Figure 7. Activity 3: Jumping, Leg Flexion and One Foot Jumping.

Activity 4 – Crouching, leg flexion and leg elevation

In this task, the subject was standing straight with both feet completely on the ground and was asked to perform 10 squats followed by 10 vertical leg flexions – moving the heel towards the gluteus- and 10 leg elevations – moving the knee towards the chest (Figure 8).
The subjects used an accelerometer located at the right hip and oriented so the y axis was pointing downward.

Figure 8. Activity 4: Crouching, Leg flexion and Leg Elevation.

In the new set of acquired signals we achieved the results reported on Table 3.

Table 3. Clustering results of the mean wave algorithm for signals with three modes.

Task	*Number of Cycles*	*Cycles correctly clustered*	*Errors*	*Misses*	*Accuracy (%)*
Synthetic	924	921	0	3	99,68
Act 1	693	692	0	1	99,86
Act 2 (Accelerometer)	175	149	7	20	85,14
Act 2 (Electromyography)	120	112	8	0	93,33
Act 3	180	154	7	19	85,56
Act 4	180	173	3	4	96,11
Total	2272	2201	25	47	96,88

We considered errors as misclassifications and misses as cycles which weren't classified at all.The misses encountered were mostly present in the borders of the signals. The clustering mechanism returned the number of cycles clustered in each group and as we knew beforehand the number of cycles per class it was possible to determine the cycles which were wrongly clustered. As can be seen from the last column, the algorithm implemented also shows a high accuracy when applied on activities with more than two modes.

That way we were able to check the performance of our algorithm when more than two clusters are involved. In the new set of acquired signals we achieved 96.88% of accuracy separating the three activities into different clusters, lowering our previous clustering result with two modes by only 2.4% and using a greater amount of cycles.

Noise Immunity Test

With the intention of performing a noise immunity test in our algorithm we added Gaussian noise of mean zero and deviation error variable to the synthetic signal that we described previously. We compared the accuracy of the algorithm with the signal-to-noise ratio (SNR) for each situation. The results for this test are detailed in Table 4.

Table 4. Noise Immunity Test. Number of cycles = 924.

Signal-to-Noise Ratio	*Cycles correctly clustered*	*Errors*	*Misses*	*Accuracy (%)*
No noise	921	0	3	99.7%
SNR = 8.00	921	0	3	99.7%
SNR = 4.00	921	0	3	99.7%
SNR = 2.67	918	3	3	99.4%
SNR = 2.00	907	14	3	98.2%
SNR = 1.33	726	195	3	78.6%
SNR = 1.00	561	360	3	60.7%

From no noise to a SNR = 2, the results of the algorithm remained stable (99.7-98.2% of accuracy). With SNR values of 1.33 and 1.00 the accuracy lowered to 78.6 and 60.7%, respectively, which are acceptable considering an amount of noise with amplitude equal or superior than the signal to analyze.

CONCLUSION

In this work we further evaluated an algorithm previously presented, which is based on a generic mean wave approach to cluster the cycles of biosignals.

Our algorithm proves to be an accurate method in the detection of changes in the signal's morphology, achieving 99.3% of clustering accuracy in signals with only two different modes or activities. The algorithm accuracy for signals with three different modes was tested in this chapter, achieving an overall result of 96.9%.

We compared our clustering procedure with another method referenced in literature, the cepstral coefficients algorithm, which presented the best results to the date for time series data. We obtained better results using the same dataset of acquired data – the mean wave algorithm presents an accuracy 19% superior for the same data. The mean wave procedure is also much more appropriate for the analysis of continuous signals, as it automatically separates the signals' cycles and doesn't need different inputs for different signal's modes, unlike the cepstral coefficients algorithm.

Finally we performed a noise immunity test with a synthetic signal, adding Gaussian noise until the clustering procedure decreases in accurateness. Only with a noise of amplitude equal to the synthetic signal and therefore a signal-to-noise ratio of 1, the accuracy of the algorithm drops to 60.7%; however, the algorithm proved to be relatively stable for a SNR higher than 2.

The necessary validation tests that we performed in this study confirmed the high accuracy level of the developed algorithm for biosignals which express human behavior.

The continuously need to obtain more information, with more accuracy, more quickly and with less intervention from an expert has led to a growing application of signal processing techniques applied to biomedical data. The biosignal analysis and processing is a promising area with huge potential in medicine, sports and research.

In fact, pattern recognition and automatic classification of morphological and physiological deviations on biosignals using clustering techniques are essential on monitoring elderly people on their homes (AAL).

Thus, the mean wave algorithm is a great asset in this context and can contribute to the main goal of AAL: increase the period of time in which elderly people are autonomous by being able to detect behavior and changes in biosignals (e.g. arrhythmia, fall detection, epilepsy episodes). Concerning sports, we can identify different actions in the same data resulting in correct group detachment. This outcome provides feature extraction in order to recognize and categorize patterns. Furthermore, it allows us to create a mathematical model which is capable to classify new movements that can be directly used on talent recruitment and/or sport's training optimizations.

Our algorithm can be applied to continuous cyclic time series, capturing the signal's behavior. The fact that this approach doesn't require any prior information and its good performance in different situations makes it a powerful tool for biosignals analysis and classification.

REFERENCES

AAL4ALL – Ambient Assisted Living for All. Last accessed in February 17, 2012 at http://www.aal4all.org/?lang=en.

Antoniol, G., Rollo, V., and Venturi, G., Linear predictive coding and cepstrum coefficients for mining time variant information from software repositories. *MSR2005: International Workshop on Mining Software Repositories*, 2005.

Bagnal, A. and Janacek, G., Clustering time series from arma models with clipped data. In *Procedings of KDD '04, the tenth ACM SIGKDD international conference on Knowledge discovery and data mining*, Seattle, USA, Aug. 2004.

Boets, J., Cock, K., Espinoza, M., and Moor, B., Clustering time series, subspace identification and cepstral distances. *Communications in Information and Systems,Vol. 5, No. 1*, pages 69–96, 2005.

Kalpakis, K., Gada, D., and Puttagunta, V., Distance measures for accurate clustering of arima time-series. In *Procedings of the 2001 IEEE International Conference on Data Mining*, pages 273–280, 2001.

M. Corduas and D. Piccolo.Time series clustering and classification by the autoregressive metric.*Computational Statistics & Data Analysis, Vol 52*, pages 1860–1872, 2008.

Nunes, N., Araújo, T. and Gamboa, H. (2012) Time Series Clustering Algorithm for Two-Modes Cyclic Biosignals. In A. Fred, J. Filipe, and H. Gamboa (Eds.): BIOSTEC 2011, CCIS 273, pp. 233--245. Springer, Heidelberg.

PLUX – Wireless Biosignals, S.A. Last accessed in February 15, 2012 at www.plux.info.

Physionet – PhysioBank Archive Index. Last accessed in February 15, 2012 at http://www.physionet.org/physiobank/database.

Rodrigues, G., Alves, V., Silveira, R., Laranjeira, L., "Dependability analysis in the Ambient Assisted Living Domain: An exploratory case study," The Journal of Systems and Software 85 (2012) 112–131

Santos, R., Sousa, J., Sañudo, B., Marques, C., Gamboa, H., "Biosignals Events Detection A Morphological Signal-Independent Approach," Proceedings of the International Conference on Bio-inspired Systems and Signal Processing (BIOSIGNALS 2012), Vilamoura, Portugal, 2012.

Savvides, A., Promponas, V. and Fokianos, K.., Clustering of biological time series by cepstral coefficients based distances. *Pattern Recognition, Vol 41*, pages 2398– 2412, 2008.

Souza., P. Statistical tests and distance measures for LPC coefficients. *IEEE Transactions on Acoustics, Speech and Signal Processing, Vol 25, Issue 6*, pages 554–559, 1977.

Key Terms & Definitions

Mean wave: Having a set of signal's cycles, the mean wave is a wave constructed by the mean value for each time-sample of those cycles.
Clustering: A method for assigning an observation to a specific group of observations which share some characteristics, differentiating them from others.
Biosignals: The human body produces physiological signals which can be measured. To those signals we call "biosignals".

Human Activity Recognition for an Intelligent Knee Orthosis

Diliana Rebelo[1], Christoph Amma[2], Hugo Gamboa[1,3] and Tanja Schultz [2]
[1] *CEFITEC, Physics Department, FCT-UNL, 2829-516, Caparica, Portugal*
[2] *Cognitive System Lab (CSL), Karlsruhe Institute of Technology (KIT), Germany*
[3] *PLUX-Wireless Biosignals, S.A, 1050-059, Lisbon, Portugal*
dm.santos@campus.fct.unl.pt, christoph.amma@kit.edu, hgamboa@plux.info, tanja.schultz@kit.edu

Keywords: Biosignals, Human activity recognition, Signal-processing, Hidden Markov Models

Abstract: This paper investigates the possibility to classify isolated human activities from biosignal sensors integrated into a knee orthosis. An intelligent orthosis that is capable to recognize its wearers activity would be able to adapt itself to the users situation for enhanced comfort. We use a setup with three modalities: accelerometry, electromyography and goniometry to measure leg motion and muscle activity of the wearer. We segment signals in motion primitives and apply Hidden Markov Models to classify these isolated motion primitives. We discriminate between seven activities like for example walking stairs and ascend or descend a hill. In a small user study we reach an average person-dependent accuracy of 98% and a person-independent accuracy of 79%.

1 INTRODUCTION

Passive orthoses are widely used for conservative therapy of diseases like Gonarthrosis, which is Osteoarthritis in the knee joint. Depending on the type of arthrosis, these orthoses apply a constant force on the knee joint to correct a defective position. This is usually painful or at least unpleasant for the wearer after a certain amount of time. Future active orthoses could be able to vary this force depending on the current wearers activity and therefore only apply force if the knee joint is stressed, e.g. while walking stairs but not while the wearer is sitting. This will impose less strain on the wearer. In order to develop such a system, it will be necessary to recognize the wearers activity, which is the topic of this paper. The study presented in this paper is part of a larger effort to develop such active orthoses.

In this paper we evaluate the possibility to recognize human activities based on data from biosignal sensors solely placed on or under an existing passive knee orthosis to allow future integration of sensors. The contribution of this paper is the evaluation of the ability to recognize activities with these restrictions on sensor placement as well as providing a proof-of-concept for the development of an activity recognition system for an intelligent orthosis.

The focus of this work is the question how well we can discriminate already segmented isolated motion primitives. In case of periodic activities like walking, we define a primitive as one cycle, in case of non-periodic activities like sitting down, we define a primitive as the complete motion. Therefore, prior to classification, the continuous data recordings need to be segmented into isolated motion primitives. We use an automatic approach for the segmentation of all periodic activities and perform manual segmentation for non-periodic activities. We use Hidden-Markov-Models (HMM) as classifier and model each of the seven motion primitives with one HMM. In future work we want to rely on the implicit segmentation ability of HMMs to allow for realtime usage.

2 RELATED WORK

Gait and posture are often categorized as the standard human movement from which analysis allow clinical evaluation. In the past, some studies have proved the reliability of accelerometry on activity recognition on data collected from different areas of the body. For example, in (Mathie et al., 2003), the use of triaxial accelerometers successfully distinguished between activity (transitions sit-to-stand and stand-to-sit and walk) and rest. In the context of physical activity recognition, in (Welk and Differding, 2000), sedentary activities such as sitting or sleeping are discriminated from moderate intensity activities

such as walking through the analysis of acceleration data.
The use of EMG or electrogoniometers have been applied mostly on kinematics evaluation (Rowe et al., 2000) or on pattern comparisons for diagnosis (Suda, 2011).
However, these aforementioned researches use only accelerometers, goniometers or EMG sensors separately with less restrictions on sensor placement.

Hidden Markov Models (HMM) are widely used for activity recognition (Lukowicz et al., 2004). They are especially useful if motions can be modeled as a sequence of motion primitives like for example gestures from a gesture alphabet (Amma et al., 2012).

3 DATA ACQUISITION AND SIGNAL PROCESSING

3.1 Experimental Setup

We equipped a standard Ortema[1] ipomax passive orthosis with two triaxial accelerometers and one biaxial goniometer. Additionally, six EMG sensors to measure muscle activity were put on the skin under the orthosis. It is a requirement of our application scenario to place all sensors on or under the orthosis, since all sensors should be integrateable into the orthosis in the future. The orthosis itself consists of two rigid shells, one for the upper and one for the lower leg which are fixed to the leg with straps. The shells are connected by a joint on each side in order to allow flexion of the knee joint. The accelerometers were placed on the frontside of the orthosis, one on the lower part and one on the upper part to measure acceleration of tibia and femur respectively. The goniometer was placed on the joint so it can measure the angle of the orthosis joint which can be assumed equal to the angle of the knee joint. Although the goniometer is biaxial only the axis aligned to the rotation axis of the orthosis joint was used. EMG electrodes were placed on the knee's main extensor and flexor muscles: *semimembranosus*, *semitendinosus*, *gastrocnemius* (external and internal), *vastus lateralis* and *vastus medialis*. Figure 1 shows the EMG electrodes' locations (A, B) as well as the complete experimental setup (C).

The signals were recorded wirelessly with two synchronized bioPluxresearch[2] devices at a sampling rate of 1000 Hz.
We performed a study with 6 healthy male subjects in the age between 20 and 30. Although the orthosis was not adapted to the anatomy of the subjects, all participants were able to move their knee freely and didn't feel any pain. Additionally, we made video recordings of the experiments for reference.

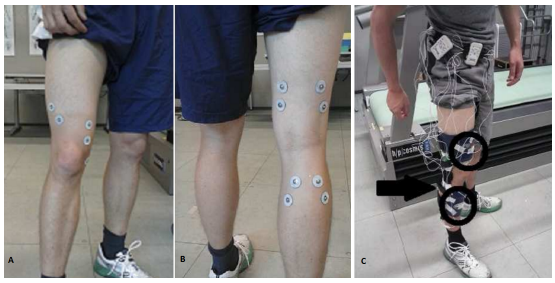

Figure 1: (A, B) Placement of electromyography surface electrodes (C) Complete experimental setup: two Bioplux research devices, two ACC (circles), six EMG and one goniometry sensors (arrow) placed on a regular Ortema right knee orthosis

3.2 Acquisition Protocol

The subjects performed the following 7 activities for the given number of repetitions:

- **Activity 1.**: Sit and stand (20 repetitions);
- **Activity 2.**: Sit, stand and walk a few steps (5 repetitions);
- **Activity 3.**: Walk to a chair, turn, sit and stand (20 repetitions);
- **Activity 4.**: Walk and stairs up (10 repetitions);
- **Activity 5.**: Walk and stairs down (10 repetitions);
- **Activity 6.**: Ascend a hill (2 repetitions of 2 minutes each, with 27% of inclination);
- **Activity 7.**: Descend a hill (2 repetitions of 2 minutes each, with 27% of inclination);

Activities 6 and 7 were performed on a treadmill with an adjustable inclination at a walking speed of 2.5 km/h.
The combined activities were chosen to have more challenging data for future evaluation of continuous recognition of activities. Since this is not in the scope of this paper the recorded data was segmented into motion primitives. In total, we work with 7 movements: *walk* (W), *stand-to-sit* (St), *sit-to-stand* (Si), *stairs up* (Su), *stairs down* (Sd), *ascend* (A) and *descend* (D).

[1] www.ortema.de
[2] www.plux.info

3.3 Data Segmentation

The purpose of the data segmentation step is to split the continuous sensor recordings into motion primitives. For the periodic motions *walk*, *stairs up*, *stairs down*, and *ascend* and *descend* a hill, we define a motion primitive as one complete gait cycle. For motions like *stand-to-sit* and *sit-to-stand*, we define a motion primitive as the movement that occurs between the two static postures "stand" and "sit". We segment each continuous periodic signals in its unique motion primitives. We segment the periodic activities according to the standard segmentation of gait cycles in (Sutherland, 2002). A gait cycle consists of a stance and a swing phase and starts and ends with the initial contact of the heel on the floor. At this point of the gait cycle the knee angle is minimal.

For cyclic motions we compute the minima of the goniometer signal and take these as segment borders. Figure 2 illustrates the resulting segmentation. The

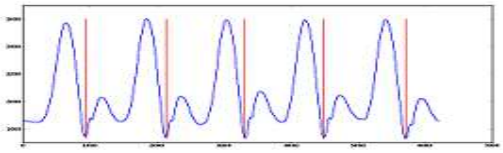

Figure 2: Example segmentation of the activity *walk* shown for the goniometer signal. The minima represent segment borders.

non-periodic movements *stand-to-sit* and *sit-to-stand* were segmented manually based on the goniometer signal. We visually checked the results of the automatic segmentation to verify the correctness of our data segmentation.

3.3.1 Data corpus

After acquisition and segmentation of all recorded data, the segments for the seven different activities form our data corpus. In order to get a balanced dataset for the evaluation we randomly chose 17 segments per person for each activity, which is the minimum number of samples we recorded over all activities. The resulting balanced data corpus therefore consists of 119 segments per person and 714 segments in total.

3.4 Classification and Feature Extraction

For feature extraction, the signal is windowed using a rectangular window function with 50 ms window length and no window overlap. All features are computed on the resulting windows. We denote the samples in one window by $(x_1,\ldots,x_N)$ where N is the total number of samples per window. Along the experiments, for each window, we extract the *Average* $avg = \frac{1}{N}\sum_{k=0}^{N-1} x_k$ for the goniometer and accelerometer's output and the *Root Mean Square (RMS)* $RMS = \sqrt{\frac{1}{N}(x_1^2+x_2^2+\ldots+x_N^2)}$ for the EMG signals.

We use continuous density Hidden Markov Models (HMM) as classifier (Rabiner, 1989). Each motion primitive is modeled by one HMM with a left-to-right topology with 10 states and Gaussian-Mixture-Models with two components. In future work we want to evaluate the ability to concatenate the primitive models to recognize continuous activities without the need for explicit segmentation. We use the BioKit toolbox developed at the Cognitive Systems Lab for the HMM training and decoding.

4 EXPERIMENTS

We evaluate the classification accuracy for classifying isolated motion primitives for all modality combinations in a subject-dependent and a subject-independent context.

4.1 Experiment 1: Subject-dependent

To evaluate the subject-dependent accuracy of the classifier we performed a leave-one-out cross-validation for each subjects data. We reach accuracies between 65% and 98% depending on the signal modalities used. Table 1 shows the results from which we can state that the combination GON&ACC has the highest accuracy.

Table 3 shows the confusion matrix for the best performing signal combination GON&ACC.

Table 2 shows the classification accuracy per subject for the best set. High accuracies are reached for all subjects. For the subject-dependent case, we believe that a robust activity recognition is possible.

	Classification Accuracy (%)	
	Subject dependent	**Subject independent**
EMG	65.41 ± 0.17	44.57 ± 13.87
GON	83.33 ± 0.12	61.46 ± 11.67
ACC	97.34 ± 0.01	75.05 ± 22.65
EMG&GON	72.13 ± 0.17	47.94 ± 14.60
GON&ACC	98.32 ± 0.05	78.70 ± 21.64
EMG&ACC	81.23 ± 0.14	55.52 ± 14.46
All	87.54 ± 0.13	63.66 ± 17.14

Table 1: Classification accuracy (mean and standard deviation) per combination of signals in subject's dependent and independent context

Subjects	Classification Accuracy (%) Subject dependent	Subject independent
1	97.32 ± 0.04	36.13 ± 21.43
2	99.11 ± 0.02	83.19 ± 10.11
3	97.32 ± 0.04	89.08 ± 4.56
4	98.22 ± 0.03	78.15 ± 8.17
5	98.22 ± 0.03	94.12 ± 0.15
6	99.11 ± 0.04	91.52 ± 0.87

Table 2: Classification accuracy (mean and standard deviation) per subject for the GON&ACC set in a subject's dependent and independent context

	W	**St**	**Si**	**Su**	**Sd**	**A**	**D**
W	**95(89)**	0	0	0	3(4)	1(0)	1(7)
St	0	**100(83)**	0	0	0(17)	0	0
Si	0	1(0)	**99(83)**	0(17)	0	0	0
Su	0	0	0	**98(92)**	2(4)	0(4)	0
Sd	0(4)	0(1)	0(1)	0(9)	**98(66)**	0(1)	2(18)
A	0(1)	0	0	1(32)	0	**99(67)**	0
D	0(19)	0	0	0	1(9)	0	**99(72)**

Table 3: Confusion matrix for GON&ACC in a subject-dependent and subject-independent (between brackets) context, in percentage

4.2 Experiment 2: Subject-independent

We evaluate the subject-independent performance with a leave-one-out cross-validation on the subjects. That means we test on one subjects data and train on the data of the remaining subjects. We use all samples in our database, resulting in 595 samples for training and 119 samples for testing for each subject.
We reach accuracies between 49% and 79% for the different signal modalities. Table 1 shows the results and, analogously to the subject-dependent evaluation, we can state that the combination GON&ACC has the highest accuracy. Nevertheless, compared to the subject-dependent case, the accuracy is much lower which can be explained by the variations in human motion for different subjects.
Table 3 shows the confusion matrix for GON&ACC. We can see that the movements *stairs down* and *ascend* are easily confused with *descend* and *stairs up*, respectively. This is not surprising since the performed motions are very similar for these pairs of activities.
Table 2 shows the classification accuracy per subject for the GON&ACC set.

Concerning the evaluation per subject, the recognizer performed with an accuracy between 36% and 94% with an average of 79%. Due to the small number of subjects, the generalization ability of the classifier is relatively low and thus we can see a low performance for subject 1.

5 CONCLUSION

In this work we evaluated the possibility to recognize human activities from different biosignal sensors. We reach a person-dependent accuracy of 98% and a person-independent accuracy of 79%. The combination of GON&ACC signals gives the highest accuracy. Based on the dataset and the models for the motion primitives acquired in this work, we will investigate continuous recognition of activities in the future, which will be the next step towards an active intelligent knee orthosis.

6 ACKNOWLEDGEMENTS

We would like to thank the KIT Sports Institute for their support, Plux for supplying biosignal sensors and the volunteers for the participation.

REFERENCES

Amma, C., Georgi, M., and Schultz, T. (2012). Airwriting: Hands-free mobile text input by spotting and continuous recognition of 3d-space handwriting with inertial sensors. In *Wearable Computers (ISWC), 2012 16th International Symposium on*, pages 52–59. IEEE.

Lukowicz, P., Ward, J., Junker, H., Stger, M., Trster, G., Atrash, A., and Starner, T. (2004). Recognizing workshop activity using body worn microphones and accelerometers. In *Pervasive Computing*, volume 3001 of *Lecture Notes in Computer Science*, pages 18–32. Springer.

Mathie, M., Coster, A., Lovell, N., and Celler, B. (2003). Detection of daily physical activities using a triaxial accelerometer. *Medical and Biological Engineering and Computing*, 41(3):296–301.

Rabiner, L. (1989). A tutorial on hidden markov models and selected applications in speech recognition. *Proceedings of the IEEE*, 77(2):257–286.

Rowe, P., Myles, C., Walker, C., and Nutton, R. (2000). Knee joint kinematics in gait and other functional activities measured using flexible electrogoniometry: how much knee motion is sufficient for normal daily life? *Gait & posture*, 12(2):143–155.

Suda, E. (2011). Análise eletromiográfica comparativa de tornozelo durante a aterrissagem em jogadores de vôlei com instabilidade crônica.

Sutherland, D. (2002). The evolution of clinical gait analysis: Part ii kinematics. *Gait & posture*, 16(2):159–179.

Welk, G. and Differding, J. (2000). The utility of the digiwalker step counter ro assess daily physical activity patterns. *Medicine and Science in Sports and Exercise*, 9(32):481–488.